6. Instrumentation

Session 8

Brighton Conference Proceedings 2005, R. Holmberg et al

The measurement and analysis of detonation pressure during blasting

S. Mencacci
Nitrochimie, EPC Group, St-Martin-de-Crau, France

R. Chavez
Nitro-Bickford, Paris, France

ABSTRACT: The Industrial Explosives Division of the EPC Group has an ongoing research programme concerned with the monitoring and analysis of detonation pressure induced by detonation of explosives during blasting. The outcome of this work is the development of reliable monitoring technology called EXPRESS (EXplosive PRESSure), based on carbon gauge technology. Carbon resistor gauges provide a relatively inexpensive and simple method with a good accuracy for detonation pressure measurements. Detonation pressure is an important parameter for the characterization of the explosive, especially during field operations. It informs us about how the explosive energy is released during blasting. Different results with various explosives on several quarries in Europe are presented.

1 INTRODUCTION

Controls of detonation explosives parameters during blasting operations are increasingly effective, owing in part to the development of bulk explosives produced on site.

For example, velocity of detonation measurements are very common. This paper deals with a complementary method based on carbon gauges technology for detonation pressure measurement in the hole.

We will present first the pressure system and the calibration operations. In a second part, we will see examples of different pressure curves measured on several quarries in Europe. Finally, in a third part, we will discuss on how these results could be used for the determination of the explosive energy released by explosive during blasting.

2 PRESSURE MEASUREMENT SYSTEM

The Industrial Explosives Division of the EPC Group has developed a reliable monitoring technology called EXPRESS (EXplosive PRESSure) (see Fig. 1), based on carbon gauge technology for detonation pressure measurement induced by detonation of explosives during blasting operations.

Carbon resistor gauges have been shown in the past to provide a relatively inexpensive and direct method, with a good accuracy for pressure measurements (Ginsberg & Asay 1991).

Wieland (1988) used carbon gauges to measure interhole blast pressures, which he believed to be the cause of observed malfunction in underground coal blasts.

Figure 1. EXPRESS system.

Katsabanis (1993 & 1994) used carbon gauges to explore detonator and explosives malfunction, as well as pressure transmission through various inert decking materials.

Mencacci (2003) has studied the origins and effects of interdeck pressure in decked blasts with pressure measurement made with carbon gauges.

The gauge (see Fig. 2) is fabricated by coating the carbon resistor (510 ohms, 0.125 W) into a suitable plastic material. When subjected to a strong shock wave, the gauge undergoes compression and the conductivity increases in proportion to the magnitude of the pressure. The transducer driving circuit provides a constant source voltage regardless of the load.

Figure 2. EXPRESS carbon gauge.

The EXPRESS system is equipped with two channels. The case prevents damage from adverse operating conditions such as temperature, shock, vibration and harsh weather conditions.

The levels of pressure that can be measured range from 5 to 140 kbar. Output is via external connectors giving a voltage that relates to the pressure value. This voltage can be recorded on any suitable oscilloscope or other data capture devices with a minimum sampling frequency of 50 MHz.

3 SYSTEM CALIBRATION

Initial calibration is carried out at Nitrochimie's facility in the south of France. The signal is recorded with an oscilloscope and converted to pressure, in kbar, by the application of a calibration curve.

Unconfined cylinder tests are used to investigate a large pressure range (5–140 kbar) with a combination of different ideal high explosives and inert materials at the back. A carbon resistor gauge is included on the bottom of the attenuator.

High explosives used are PETN and nitromethane. Thick attenuators used are Plexiglas, copper, aluminium and steel.

Figure 3 shows a schematic of the carbon resistor test set-up.

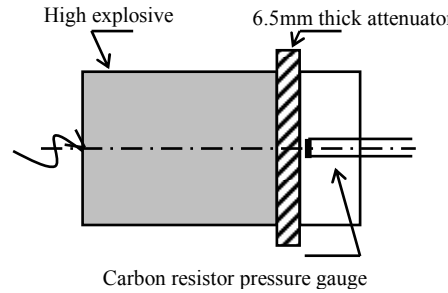

Figure 3. Calibration set-up.

The relative conductance shift is defined by

$$\mathrm{RCS} = R_{\min}/R_0$$

where RCS = relative conductance shift; R_0 = initial gauge resistance; and R_{min} = resistance of gauge under pressure. Figure 4 shows the calibration curve obtained for the EXPRESS system.

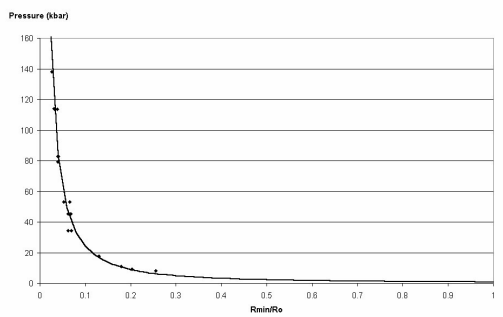

Figure 4. EXPRESS calibration curve.

3.1 Reproducibility

In order to establish the reproducibility of the measure, we have compared the pressure generated by the couple nitromethane/steel.

This test was repeated 3 times, and a comparison of the three signals was made. The results are shown in Figure 5, and it can be seen that the three traces show very good agreement. The rise time of the sensor is around 300 µs.

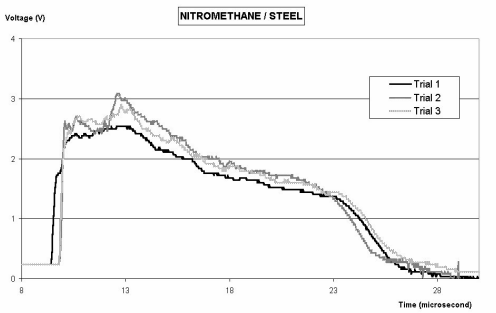

Figure 5. Results of reproducibility test.

4 PRELIMINARY TRIAL RESULTS

A series of preliminary field trials have been undertaken employing the EXPRESS system. These trials have been aimed at investigating the detonation pressure of different explosives in various conditions.

4.1 Case study 1 : cartridged explosives

In order to compare the performance of cartridged explosives, different trials were done with dynamites and emulsion products.

The gauge was placed above the top of the explosive charge as shown in the hole loading diagram given in Figure 6. The diameter of the explosives cartridges used was 50 mm, and the hole diameter was 76 mm. The ground in which the blast took place was saturated with water so that the test hole had water to collar level.

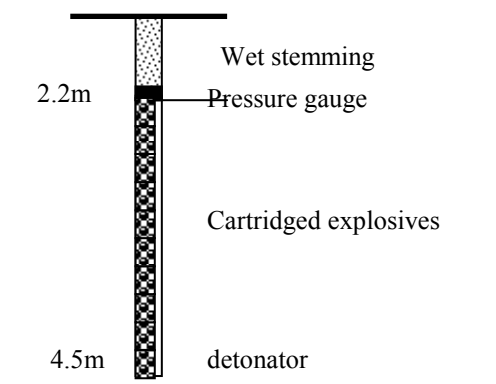

Figure 6. Hole loading diagram for case study 1.

From Figure 7 it can be seen that pressure for the dynamite product rises rapidly to a peak of 120 kbar. In contrast, for the emulsion product, the pressure rises to a maximum of 100 kbar.

These results are logical, because maximum pressure is directly related to velocity of detonation (VoD). For dynamite VoD= 6500 m/s, and for emulsion VoD = 5000 m/s in these conditions.

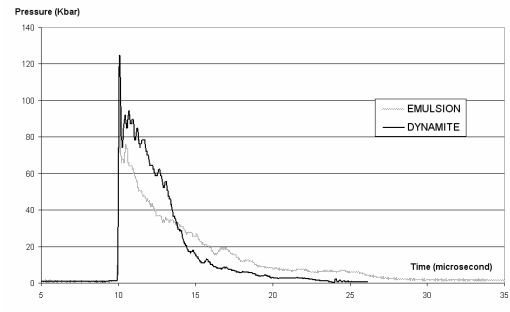

Figure 7. Pressure trace for case study 1.

Approximately 4 µs after the peak pressure, it can be seen that the pressure is higher for the emulsion product. This is certainly due to the kinetic reaction which is slower for emulsion than for dynamite.

The slower the reaction kinetics, the lower is the energy released in the detonation front. Consequently, the energy released after the shock front, essentially in the form of gases, is higher, leading to a greater pressure for emulsion. For more details about the influence of the kinetic reaction, see Bleuzen (2003).

4.2 Case study 2 : ANFO in the blasthole

A pressure gauge was installed in the blasthole loaded with ANFO explosive, as shown in Figure 8. The burden in this case was 4 m, the spacing 4.5 m and the hole diameter was 95 mm.

The blast consisted of three rows of holes and was fired with electronic detonators. All the blastholes were dry.

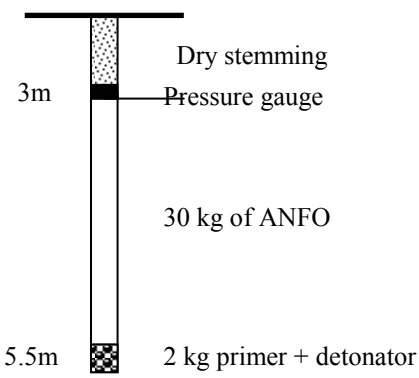

Figure 8. Hole loading diagram for case study 2.

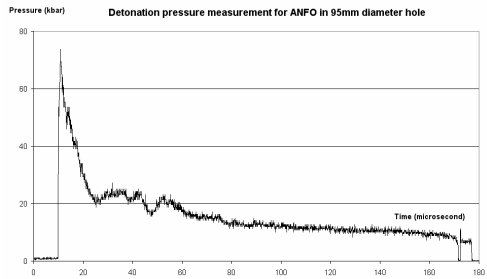

Figure 9. Pressure trace for case study 2.

Figure 9 shows the pressure recording by the gauge.

It can be seen that the pressure rises rapidly to a peak of around 74 kbar. This value is lower than those obtained for dynamite and emulsion products. Indeed, for the same reasons as previously, the velocity of detonation of ANFO in these conditions is nearly 3800 m/s.

At 12 µs after the peak pressure, the pressure is around 20 kbar, with a slow decrease to 10 kbar at 150 µs after the peak.

When we compare this curve with that obtained for a steel tube with the same diameter and product, we observe similar pressure during the first 12 µs. On the other hand, the second part of the curve is very different. With the steel tube, the pressure decreases rapidly to 0 kbar.

This means that the slower decrease in pressure in the blasthole for ANFO during the first 150 µs is certainly due to pressure maintained by the rock confinement.

4.3 Case study 3 : different diameters of heavy ANFO explosives

4.3.1 ANFO in different diameters

In order to compare the influence of the diameter, we have made a comparison for ANFO in two different diameters: 95 and 110 mm.

Figure 10 shows the pressure recordings by the gauges.

It can be seen that the pressure for 110 mm rises rapidly to a peak of 83 kbar. In contrast, pressure for 95 mm rises to 74 kbar.

These results are logical because, as said before, maximum pressure is directly related to velocity of detonation. And it is well known that, when the hole diameter increases, the velocity of detonation of explosives such as ANFO increases.

During the first 20 µs, the pressure is higher for 110 mm.

At 50 µs after the peak pressure, we observe a rapid decrease for the 110 mm signal, which is due to the destruction of the gauge.

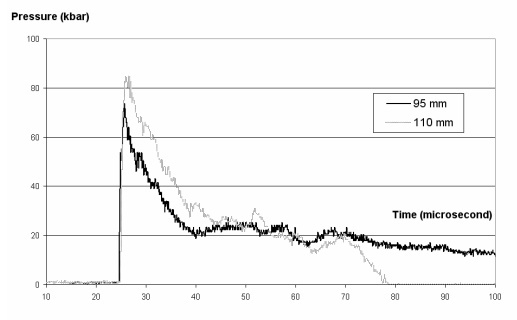

Figure 10. Pressure trace for case study 3.1.

4.3.2 Two heavy ANFOs of the same diameter

In this case, we have compared two different heavy ANFOs produced with the same multiblend truck.

The bench height was 15 m, the burden was 5 m, the spacing was 4.5 m and the hole diameter was 165 mm. The rock type was Dolomie.

A summary of the explosive data is given in Table 1.

Table 1. Summary of explosive data for case study 3.2.

Explosive name	Matrix emulsion	ANFO	Global kinetic reaction	Type
Blendex 30	30 %	70 %	'Slow'	Augered
Blendex 70	70 %	30 %	'Rapid'	Pumped

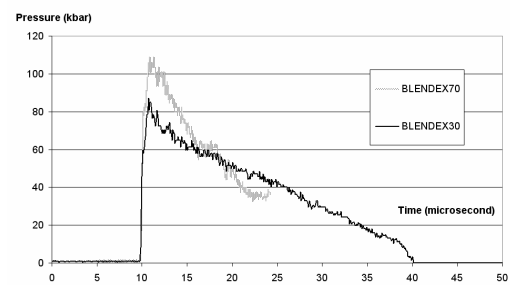

Figure 11. Pressure trace for case study 3.2.

Figure 11 shows the pressure recordings for the gauges.

It can be seen that the pressure for Blendex 70 rises rapidly to a peak of 110 kbar. In contrast, for Blendex 30, the pressure rises to a peak of 84 kbar.

As said before, these results are related to the velocity detonation records. Indeed, the VoD for Blendex 70 in these conditions is 5500 m/s, and 4500 m/s for Blendex 30.

The second part of the curves is very surprising –two different decreases in pressure are observed. This is mainly due to the very different reaction kinetics of the two explosive products. Blendex 30, which contains mainly ammonium nitrate in prills, has a 'slow' reaction kinetics. Therefore, the energy is released slowly. In contrast, Blendex 70 has a 'rapid' reaction kinetics and the energy is released rapidly.

5 DISCUSSION

The method has proven to be an inexpensive and reliable technology for controlling explosive detonation in the field. It gives insight into the pressure release over time, and thus provides more information concerning the action of detonation to the surrounding medium. The VoD can be correlated to the first pressure peak on the pressure–time curve. Consequently, detonation pressure measurements are a step forward compared with traditional VoD measurements.

Field and laboratory tests have shown that, even though detonation pressure curves last for tens of microseconds only, they show a very different behaviour from one explosive to another. These tests made it possible to distinguish between rapid kinetics and slow kinetics explosives. The former, in spite of a high initial pressure peak, show a quick decrease in the pressure curve. The latter show a slower decrease in the pressure curve, sustaining pressure for longer. One of the consequences is that explosives with the same potential energy may have a different effect on the surrounding rock. The efficiency of explosives can be affected by this different behaviour.

Furthermore, the time–pressure curve will not only depend on the kind of explosive but also on the blasting conditions. The type of rock (different harnesses) and also the borehole conditions, as the explosive comes into contact with rock, air or water, can influence the pressure release. Local static pressure or transient pressure, mainly caused by detonation of neighbouring holes, can also have a great influence on explosive efficiency. Field detonation pressure measurements are a good means to characterize the disturbance induced by all these phenomena. The expansion of the database of information by means of EXPRESS measurements could allow better prediction of the behaviour of explosives in the field.

As energy can be correlated with the integral of the pressure curve, this could represent a further step in explosive characterization. The concept of a static and constant explosive energy could be replaced by actual values of energy release, according to different blasting conditions. Some explosives with an equivalent potential chemical energy could turn out to be more sensitive to local field conditions and thus be less efficient or reliable.

Modern blasting techniques are aimed at precisely adapting explosive energy to actual field conditions. This is based on precise assessment of geometrical variations and local rock characteristics. These methods will be more efficient if sufficient knowledge of the actual explosive energy release is available. For practical purposes, the method could replace traditional quantification methods such as chemical energy content or aquarium test measurements. EXPRESS will probably have to be combined with pressure measurements at the explosive–hole interface, in order to quantify actual transmitted energy to the rock.

6 CONCLUSION

A reliable system has been developed for the monitoring of pressure detonation measurements. The system has the advantage of using relatively cheap pressure sensors, thus allowing large numbers of monitoring exercises to be carried out in an economic fashion.

The EXPRESS technology provides more information on the energy release over time and represents a further step in explosive field control. Field tests have shown significant differences between explosives in terms of amplitude and duration of the pressure curve. These differences certainly affect the energy transmission to the surrounding rock. At the same time, detonation pressure curves are affected by surrounding conditions and make it possible to compare the actual energy release depending on variable field parameters.

The detonation pressure technique already comprises a new method for better explosive characterization. This characterization is based not only on the potential energy that explosives may deliver but also on their actual efficiency in relation to implementation in the field.

Fieldwork continues to be undertaken to expand the database of information relating to detonation pressure results.

REFERENCES

Bleuzen, Y. & Mencacci, S. 2003. Numerical modelling and evaluation of the detonation of non-ideal explosives applied to the optimization of explosive choice for blasting operations. *Proceedings of Second World Conference on Explosives and Blasting Technique, Prague, Czech Republic.*

Ginsberg, M.J. & Asay, B.W. 1991. Commercial carbon composition resistors as dynamic stress gauges in difficult environments. *Rev. Sci. Instrum.* 62(9).

Katsabanis, P.D. & Yeung, C. 1993. Effects of low amplitude shock waves on commercial explosives – the sympathetic detonation problem. *Proceedings of the Fourth Symposium on Rock Fragmentation by Blasting – Fragblast-4, Vienna, Austria.*

Katsabanis, P.D., Yeung, C., Fritz, G. & Heater, R. 1994. Explosives malfunction from sympathetic detonation to shock desensitization. *Proceedings of Tenth Symposium on Explosives and Blasting Research, Austin, Texas.*

Mencacci, S. & Farnfield, R. 2003. The measurement and analysis of near-field pressure transients in producing blasting. *Proceedings of Second World Conference on Explosives and Blasting Technique, Prague, Czech Republic.*

Mencacci, S., Lefrancois, A., Grouffal, J.Y. & Bouinot, P 2003. Temperature and pressure measurements comparison of the aluminized emulsion explosives detonation front and products expansion. *Proceedings of the Second World Conference on Explosives and Blasting Technique, Prague, Czech Republic.*

Wieland, M. 1988. Cross borehole stress wave measurement in underground coal. *Proceedings of Fourth Mini-symposium on Explosives and Blasting Research, Anaheim, California.*

Brighton Conference Proceedings 2005, R. Holmberg et al

The importance of proper seismometer coupling

R.M. Wheeler
White Industrial Seismology, Inc., Joplin, Missouri, USA

ABSTRACT: In recent years the issues of seismograph calibration and accuracy have been major focal points of the ISEE Blast Vibration and Seismograph Section. In fact, questions concerning the consistency and reliability of seismograph measurements essentially led to the development of this ISEE section. One of the early actions of the section involved the development of field practice guidelines for the use of seismographs. These guidelines specifically state that 'Placement and coupling of the vibration sensor are the two most important factors to ensure accurate ground vibration recordings'. This paper will address the results obtained from using different coupling methods to record vibration and airblast levels generated from production blasting in a limestone quarry. The data obtained clearly indicate that seismometer burial provides the best coupling for recording ground vibrations. Microphone height has also been an issue regarding the accuracy of recorded airblast levels. The data we obtained indicate that microphone height is not a significant factor.

1 ISEE SENSOR COUPLING AND MICROPHONE PLACEMENT GUIDELINES

The recommended seismometer coupling method is primarily based on the expected acceleration level. When the acceleration is expected to be less than 0.2g, no burial or attachment is necessary. Attachment refers to bolting or gluing to a rock surface. Spiking would be recommended, however. If the expected acceleration is 0.2–1.0g, burial or attachment is preferred, although spiking may be acceptable. If the expected acceleration is greater than 1.0g, burial or firm attachment is required (from USBM RI 8506).

The preferred microphone height is 0.9 m above the ground or within 3 cm of the ground. Other heights may be acceptable for practical reasons. (ANSI S12.18-1994, ANSI S12.9-1992/Part 2) (USBM RI 8508).

2 SEISMOGAPHS AND METHODOLOGY

For field tests, the seismographs used were Mini-Seis 1.0M models. These instrument types meet or exceed the ISEE seismograph performance guidelines.

The three types of measurement method employed were burial, surface spiking with a sandbag and no coupling. Burial involved digging a hole to a depth of approximately 3 times the height of the seismometer package. The seismometer package was then spiked in the ground and the soil was compacted around the seismometer. For surface spiking, an area was cleared to allow the seismometer to be spiked in the soil without any intervening grass or sod. A loosely filled 4.5 kg sandbag was then placed evenly on top of the seismometer. The third method involved clearing an area and then simply placing the seismometer on the ground with no spiking or sandbag.

3 FIELD TESTS

For the purposes of this investigation, a series of limestone quarry production blasts were monitored using 2–3 seismographs per blast. The seismographs were placed close together. Each unit was set up using one of the seismometer coupling methods noted previously. Varying microphone heights were also used. Measured vibration levels covered a wide range.

3.1 Field test 1

Three seismographs were used during the first test.

The distance to the blast was approximately 200 m. The seismometer for seismograph 1 was buried and the microphone was mounted 0.9 m off the ground. The seismometer of seismograph 2 was spiked and sandbagged and the microphone was mounted 0.3 m off the ground. The seismometer and microphone for seismograph 3 were simply placed on the ground. No seismometer coupling was used. The seismograph layout is shown in Figure 1. The measurements recorded are listed in Table 1.

Figure 1. Seismograph layout.

Table 1. Data from field test 1.

	Seismo-graph 1	Seismo-graph 2	Seismo-graph 3
Radial (mm/s)	11.6	13.5	15.2
Vertical (mm/s)	18.3	19.8	37.1
Transverse (mm/s)	10.2	13.2	7.37
Acoustic (Pa)	144	148	150

Seismograph 1 with the buried seismometer recorded the lowest peak particle velocity, 18.3 mm/s. The seismograph with the spiked seismometer (seismograph 2) recorded a somewhat higher peak particle velocity with a difference of 1.5 mm/s from the buried seismometer. As would be expected, the uncoupled seismometer exhibited significantly different measurements. The peak measurement on the vertical channel was more than twice as high as the vertical measurement from the buried seismometer. The acoustic measurements showed only slight variances.

The time histories and frequency spectra of the vibrations recorded by the three seismographs are shown in Figures 2–4. There is little or no frequency energy below 10 Hz in any of the seismic spectra. It is not evident from looking at either the time history or the frequency spectra that the seismometer of seismograph 3 was not coupled.

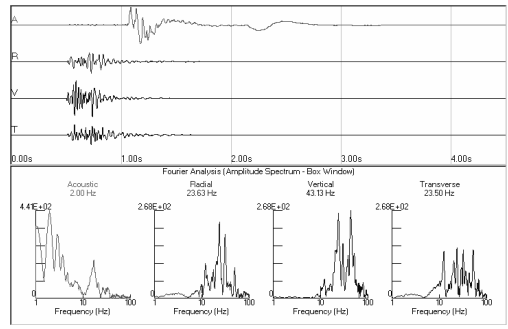

Figure 2. Seismograph 1 time history and spectra.

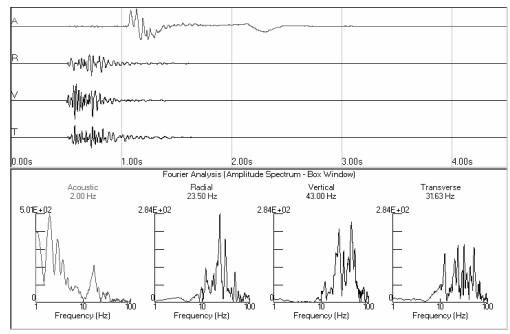

Figure 3. Seismograph 2 time history and spectra.

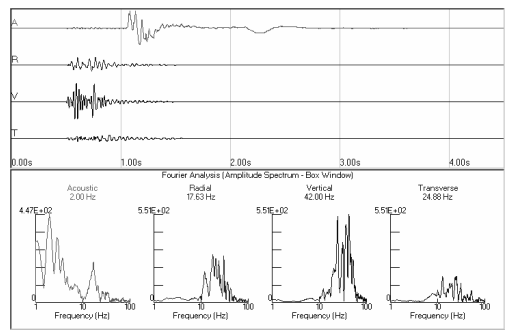

Figure 4. Seismograph 3 time history and spectra.

Since the expected acceleration is the primary factor in choosing the seismometer coupling method, we used numerical differentiation to look at the acceleration time history for the seismograph with the buried seismometer package. The vertical channel had a peak acceleration of 0.44g. For this acceleration level, the ISEE guidelines

state that burial is preferred, but spiking may be acceptable. Was spiking acceptable in this case? If we look at just the peak particle velocity, the vertical measurement was 18.3 mm/s for the buried seismometer versus 19.8 mm/s for the spiked seismometer. The difference was 1.5 mm/s.

For calibration purposes, the ISEE seismograph performance specifications require an accuracy of no worse than ±5% or a difference of no more than 0.5 mm/s, whichever is greater. Given any two seismographs, these specifications would allow a difference between the two of as much as 10% or 1.0 mm/s, whichever is greater. The difference between the two measurements is 8.3%, which is within the 10% band. Obviously, the uncoupled seismometer method was not acceptable.

Microphone height did not appear to be an issue as the maximum difference between measurements was only 4.2%.

3.2 Field test 2

Once again, three seismographs were used. The distance to the blast was approximately 230 m. The instruments were set up the same as they were for the first test. The measurements obtained are listed in Table 2.

Table 2. Data from field test 2.

	Seismograph 1	Seismograph 2	Seismograph 3
Radial (mm/s)	6.86	7.49	9.78
Vertical (mm/s)	8.64	6.99	7.37
Transverse (mm/s)	9.14	10.7	14.1
Acoustic (Pa)	112	116	126

As with test 1, seismograph 1 with the buried seismometer recorded the lowest peak particle velocity of 9.14 mm/s. The seismograph with the spiked seismometer (seismograph 2) recorded a somewhat higher peak particle velocity with a difference of 1.56 mm/s from the buried seismometer. Regarding the uncoupled seismometer, the peak measurement on the transverse channel was 4.96 mm/s higher than the transverse measurement from the buried seismometer.

The acoustic measurements from microphone heights of 0.3 and 0.9 m showed insignificant variances. The microphone lying on the ground, which is within ISEE guidelines, exhibited a 12.5% increase in peak overpressure compared with the 0.9 m microphone height.

The time histories and frequency spectra of the vibrations recorded by the three seismographs are shown in Figures 5–7. There is little or no frequency energy below 10 Hz in any of the seismic spectra. As with test 1, it is not evident from looking at the time history or the frequency spectra that seismograph 3 was not coupled.

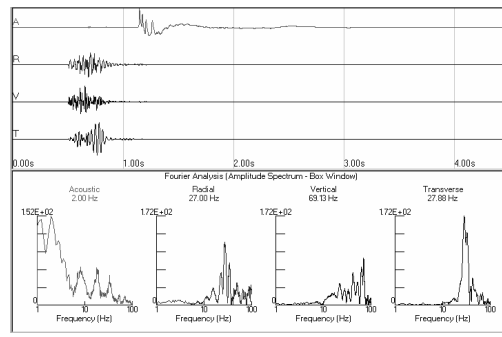

Figure 5. Seismograph 1 time history and spectra.

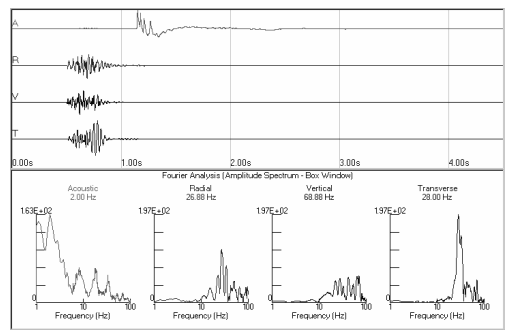

Figure 6. Seismograph 2 time history and spectra.

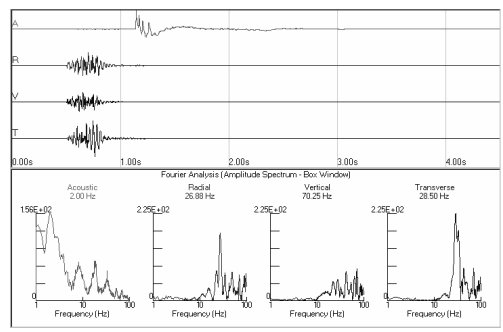

Figure 7. Seismograph 3 time history and spectra.

A peak acceleration of 0.32*g* occurred in the vertical channel. For this acceleration level, the ISEE guidelines state that burial is preferred, but

spiking may be acceptable. Was spiking acceptable in this case? If we look at just the peak particle velocity, the transverse measurement was 9.14 mm/s for the buried seismometer and 10.7 mm/s for the spiked seismometer. The difference is 1.56 mm/s. The percentage difference was 17.1% which would not fall within the 10% band. Once again, the uncoupled seismometer method was unacceptable.

Microphone height did not appear to be an issue as the maximum difference between the 0.3 and 0.9 m heights was only 3.6%.

3.3 Field test 3

As with tests 1 and 2, three seismographs were used. The distance to the blast was approximately 488 m. The instruments were set up the same as they were for the first two tests. The measurements obtained are listed in Table 3.

Table 3. Data from field test 3.

	Seismo-graph 1	Seismo-graph 2	Seismo-graph 3
Radial (mm/s)	1.14	1.27	2.29
Vertical (mm/s)	1.65	1.14	2.16
Transverse (mm/s)	1.27	0.76	1.52
Acoustic (Pa)	58	60	64

This time the lowest peak particle velocity of 1.27 mm/s was recorded with the spiked seismometer on the radial channel. The buried seismometer recorded a peak particle velocity of 1.65 mm/s on the vertical channel. The uncoupled seismometer recorded a peak particle velocity of 2.29 mm/s.

During the process of burying the seismometer, our field technician noted that he felt like the coupling in this instance was actually not as good as in the case of the seismometer that was spiked and sandbagged. We decided not to recouple the buried seismometer in order to see the results. It appears his instincts were correct.

The time histories and frequency spectra of the vibrations recorded by the three seismometers are shown in Figures 8–10. There is little or no frequency energy below 10 Hz in any of the seismic spectra. A frequency band of 20–50 Hz contains most of the energy. As with the other tests, it is not evident from looking at the time history or the frequency spectra that seismograph 3 was not coupled.

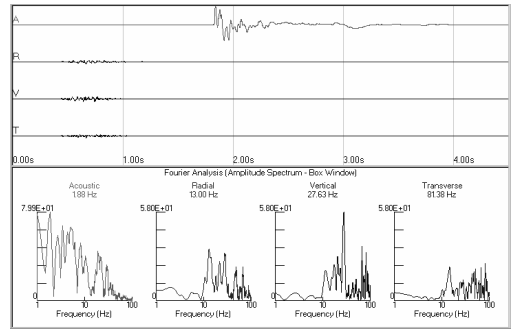

Figure 8. Seismograph 1 time history and spectra.

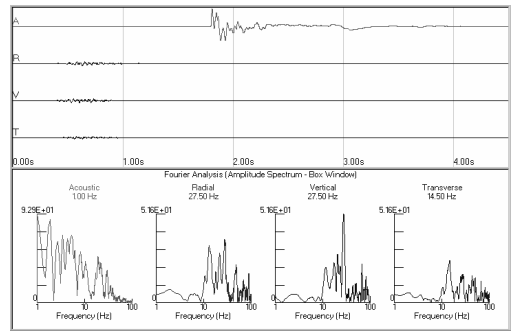

Figure 9. Seismograph 2 time history and spectra.

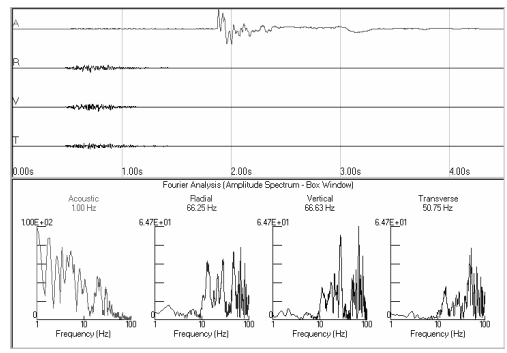

Figure 10. Seismograph 3 time history and spectra.

No acceleration analysis is needed on these data as the particle velocity amplitudes are so low. Even though the peak amplitudes occurred on different channels, the difference between the buried and spiked seismometers was only 0.38 mm/s. Once again, the peak measurement associated with the uncoupled seismometer was higher, although not as significant since the amplitude levels were low.

With tests 1, 2 and 3, the data reveal that an uncoupled seismometer is unacceptable. Burial should indeed be the preferred coupling method,

when it is able to be done properly. The next two tests involved two seismometers buried side by side.

3.4 Field test 4

In this test, three seismographs were utilized. Seismographs 1 and 2 had their seismometers buried in the same hole side by side. The seismometer for the third seismograph was spiked to the surface. Microphone heights of 0.9 m, 0.3 m and on the ground were used. The distance to the blast was approximately 145 m. The measurements obtained are listed in Table 4.

Table 4. Data from field test 4.

	Seismo-graph 1	Seismo-graph 2	Seismo-graph 3
Radial (mm/s)	26.4	29.0	40.6
Vertical (mm/s)	46.2	49.6	52.8
Transverse (mm/s)	48.3	50.3	43.2
Acoustic (Pa)	56	64	56

The two buried seismometers recorded peak particle velocities of 48.3 and 50.3 mm/s, both on the transverse channels. The seismograph with the spiked seismometer (seismograph 3) recorded a somewhat higher peak particle velocity of 52.8 mm/s on the vertical channel. The acoustic measurements showed slight variances.

The time histories and frequency spectra of the vibrations recorded by the three seismometers are shown in Figures 11–13. There is little or no frequency energy below 10 Hz in any of the seismic spectra.

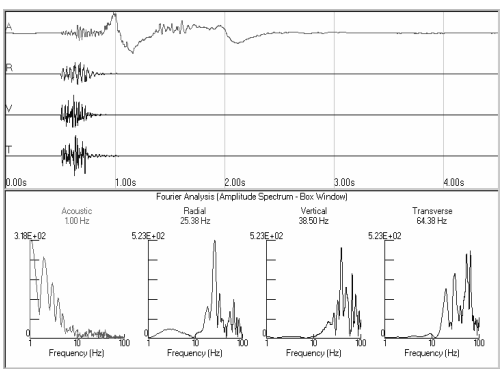

Figure 11. Seismograph 1 time history and spectra.

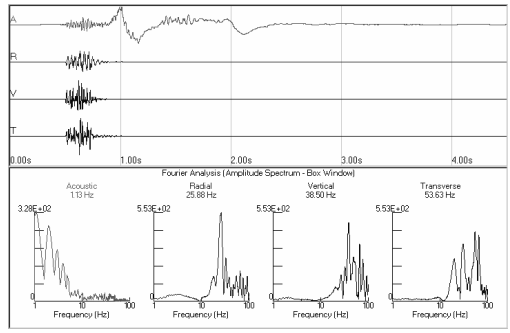

Figure 12. Seismograph 2 time history and spectra.

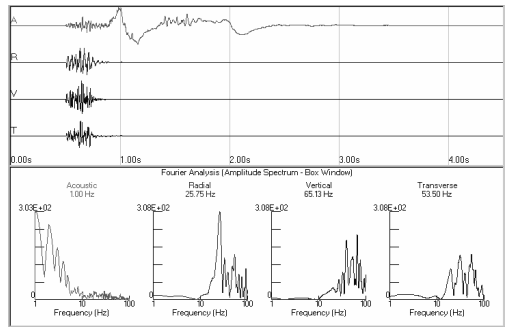

Figure 13. Seismograph 3 time history and spectra.

The peak amplitudes of the two buried seismometers are within 2.03 mm/s. There was only a 4% difference. An acceleration analysis of the transverse channel of seismograph 2 yields a peak acceleration of 1.86*g*. The ISEE guidelines require burial or attachment at accelerations exceeding 1.0*g*.

Figure 14 shows the overlaid vibration time histories and spectra for the two buried seismometers. Overlaying the data clearly reveals the differences. By cross-correlating the time histories, we can get an idea of how closely they correlate. The radial, vertical and transverse channels correlate to within 3.8, 3.4 and 7.3% respectively. A perfect correlation would have no deviation.

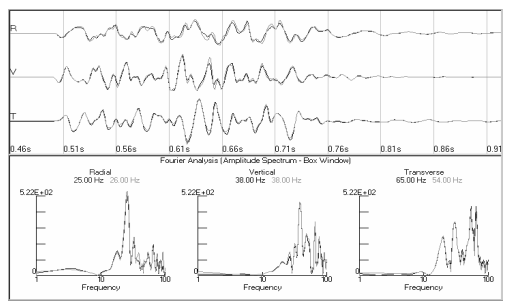

Figure 14. Overlaid data from buried seismographs.

3.5 Test 5

In the previous tests, we attempted to use good coupling methods whether burying or spiking the seismometers, but we did not go beyond what we thought would be the effort of a competent field user. For the last test, we went to great effort to achieve the best coupling we could obtain for two seismometers buried side by side in the same hole. We also selected a distance where the acceleration level would not be an issue. The purpose of this test was to attempt to obtain exact agreement in measurements. The measurements are listed in Table 5.

Table 5. Data from field test 5.

	Seismo-graph 1	Seismo-graph 2
Radial (mm/s)	1.91	1.91
Vertical (mm/s)	2.29	2.16
Transverse (mm/s)	1.78	1.78
Acoustic (Pa)	44	48

The results were almost perfect. There was a 0.13 mm/s difference between the vertical measurements. Figure 15 shows the overlaid vibration time histories and spectra for the two buried seismometers. The radial, vertical and transverse channels correlate to within 0.35, 2.25 and 2.60% respectively.

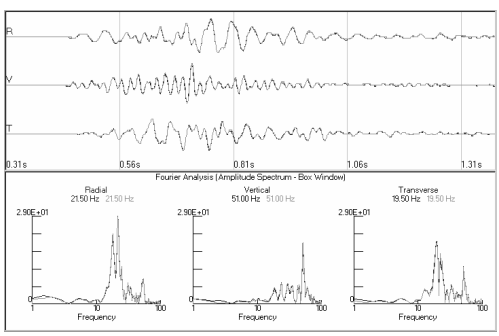

Figure 15. Overlaid seismograph data.

4 ANOTHER EXAMPLE

Depending on the frequency content of the vibrations, the higher the vibration level, the more likely it is that surface spiking may fail to provide acceptable coupling. Recently, there was a seismograph operator who contacted us and indicated that they were recording higher than expected measurements. It was discovered that they were surface spiking their seismometers with a sandbag, which was resulting in inaccurate measurements from poor coupling. The measurements over a 2 day period ranged from 65 to 193 mm/s. The average peak measurement was 140 mm/s.

Figure 16 shows the vibrations from the 193 mm/s recording. It also shows a fast Fourier transform (FFT) frequency analysis. Note the very low frequency of 1.50 Hz on the radial channel. This is a definite indication of loss of coupling. An FFT frequency analysis can possibly be useful in determining loss of coupling.

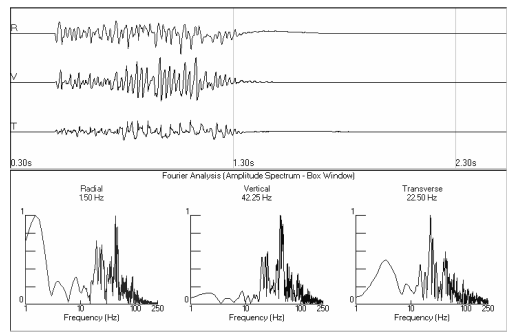

Figure 16. Seismogram showing decoupling.

Once the operator had buried the seismometer in compliance with ISEE guidelines, the measurements over the next 2 day period ranged from 57 to 93 mm/s. The average peak measurement was reduced to 82 mm/s. Coupling the seismometer properly narrowed the spread of the measurements significantly.

Figure 17 shows the vibrations from the 93 mm/s recording. It also shows an FFT frequency analysis. Note that there are virtually no significant low-frequency values.

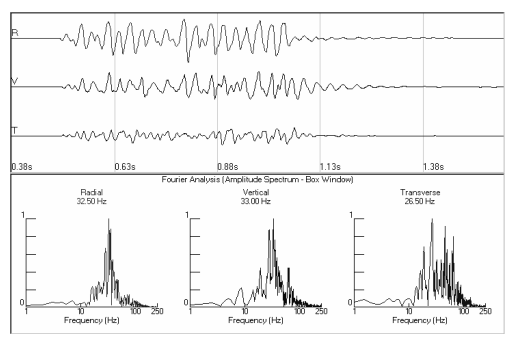

Figure 17. Seismogram after burial.

Performing an acceleration analysis of the waveform in Figure 17 by numerical differentiation yields a peak acceleration of 3.8*g*. Obviously, burial was necessary in this case in order to obtain valid measurements.

5 SUMMARY AND CONCLUSIONS

Five field tests were conducted at a limestone quarry. The tests consisted of utilizing 2–3 seismographs to record ground vibration and airblast levels utilizing different seismometer coupling methods and microphone heights.

The ISEE seismograph user guidelines recommend burial of the seismometer whenever the acceleration levels are expected to be greater than 0.2*g*. Seismometer burial is required when the acceleration level exceeds 1.0*g*. Between 0.2 and 1.0*g*, surface spiking may be acceptable. The results of our tests show that, when using surface spiking, it is very important that the area contains good competent soil. Also, it helps to have at least three points of contact either with three spikes or a baseplate/spike combination.

It is important to note that the results obtained in our test cases may or may not apply to other seismometer types. In situations where the design of the instrumentation prevents burial, extra care must be taken to achieve good coupling. With acceleration as the guideline for the proper coupling method, given a fixed particle velocity level, the issue of coupling will be different for vibrations dominated by low frequencies versus those with high frequencies.

Burial of the seismometer is not always convenient. However, convenience should not be an issue. Users sometimes call our office to question the accuracy of the instrumentation because the measurements are higher than they expect or want to deal with. Inevitably, if we check the instrument calibration, it is within ISEE performance guidelines.

There are also times when we receive a call stating that one of our instruments and another brand were set up close together but recorded significantly different measurements. The caller, of course, wants to know which instrument is incorrect. The inference is that there is an instrument accuracy problem, when it is much more likely to be a coupling issue. Keep in mind that the actual ground displacements caused by blast vibrations can be very minimal. In our test 4, the difference between the peak particle velocities of the two buried seismometers was 2.03 mm/s. However, the difference between the peak displacements on the same channel was only 0.0044 mm. Just a small amount of decoupling can manifest itself as a significant difference in particle velocity.

Regarding acoustic overpressure measurements, the ISEE requirement that the microphone height be 0.9 m above the ground or within 3 cm of the ground, never made much sense to this writer. The data presented in this work clearly indicate that microphone height is not a significant issue. The ISEE Seismograph Section is currently revisiting this issue and is expected to suggest a modification.

REFERENCES

International Society of Explosives Engineers 1998. *Blasters' Handbook*, 17th edition. Cleveland: International Society of Explosives Engineers.

Stagg, M.S. & Engler, A.J. 1980. Measurements of blast-induced ground vibrations and seismograph calibration. USBM Report of Investigations 8506: 21–22.

Brighton Conference Proceedings 2005, R. Holmberg et al

Measurement of vibration and structure-born noise with GSM support – Norrortsleden Project

J. Jonsson & S-E. Johansson
Nitro Consult AB, Stockholm, Sweden

ABSTRACT: Norrortsleden is a 16-km road project through a suburban area north of Stockholm, about 2 km of which will pass through twin tunnels underneath a large residential district. In total, about 1.1 million m^3 of rock is to be blasted, some 440 000 m^3 of it on the surface and 660 000 m^3 in the tunnels. The drill-and-blast challenge is to ensure that the levels of vibration, airborne shock waves and structure-borne noise are kept below prescribed limits. The Client, the Swedish National Road Administration (Vägverket), has appointed Nitro Consult as the drill-and-blast engineering consultant. With the aid of its UVS REMOTE and NCVIB – a system of instruments supported by GSM modems, data transfer and a dedicated Internet portal – Nitro Consult has made it easy for key personnel to read the different types and levels of disturbance quickly and safely from almost any remote location. What is more, all measurement data and blasting records can be uploaded to the Internet portal, NCVIB, which is accessible to authorized project personnel. Time-history records, too, can be read directly after each round and used to analyse different delay times, etc. This valuable information can then be used to plan subsequent rounds and optimise both the drill-and-blast pattern and the advance per round while keeping below the prescribed disturbance limits.

1 PROJECT OUTLINE

Stockholm County's northern-communities link road (Fig. 1), known locally as Norrortsleden, will improve connections between communities to the north of the city and provide a fast, safe, direct link between the E4 motorway at Häggvik and the E18 motorway at Rosenkälla, about 15-18 km north-northwest of the capital. It will form part of an outer north-south bypass to the west of the city, which will connect the county's northern and southern districts more efficiently with each other. In its entirety, the Stockholm bypass project, which may well involve an outer north-south bypass to the west of the city as well, looks set to become the largest single project ever undertaken by the National Swedish Road Administration.

The first one kilometre of Norrortsleden (called Häggviksleden) opened to traffic in September 1998. The remaining 15 kilometres, now under construction, is divided into 10 contracts.

The stretch between the communities of Edsberg and Täby will consist of an 8-km, four-lane motorway, about 2 km of which will be in tunnels (the Törnskog tunnel).

The stretch between Täby Kyrkby and Rosenkälla will consist of a 7-kilometre 2+1 collision-free road with a steel-cable barrier separating the directions of travel. About 1 kilometre of this stretch will be through a tunnel (the Löttinge tunnel), which will contain 1+1 driving lanes separated by a central wall. It shall be possible to upgrade the road to motorway standard at a later stage.

With regard to the surface and underground rock-excavation work, especially the drilling and blasting, Nitro Consult has been called in to survey the real estate around the worksite and to monitor vibration, structure-borne noise and airborne shock waves. The company is doing this with the aid of its UVS REMOTE system and dedicated Internet portal, NCVIB. Nitro Consult is also providing damage-inspection services to the client.

Here we report on the performance of the Nitro Consult system in the Norrortsleden contracts and

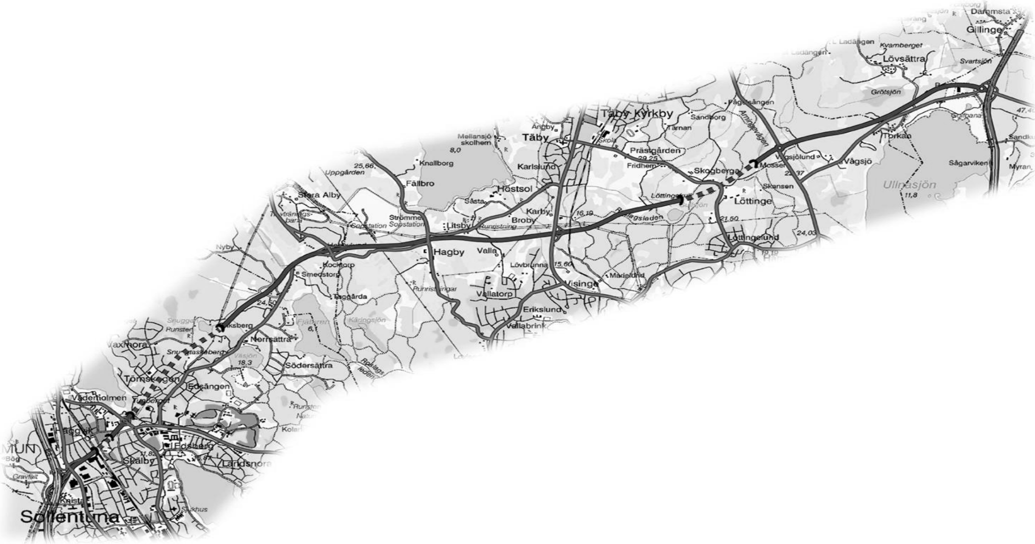

Figure 1. Map showing the route of Stockholm's northern-communities link road, Norrortsleden, about 15-18 kilometres north-northwest of the city. The sections shown with broken lines in the west and east represent the 2.1-km Törnskog and 1-km Löttinge tunnels respectively.

detail some of the measurements taken during blasting work for the Tunberget junction and Törnskog tunnel.

2 NCVIB

To facilitate the reading of vibration, airborne shock waves, noise, etc., Nitro Consult has developed a system called UVS REMOTE and NCVIB. Since all work-site offices today have good Internet connections, the system is based on communication via GSM modems in the measuring instruments, which transmit information about incoming vibrations to a measurement-data server. The server then transfers all measurement data to a dedicated, project-specific page on the NCVIB Internet portal. This saves time for contractors and builders, since they no longer have to run around reading off all the measuring points after each and every round has been fired.

The measuring instruments can also send SMS messages to up to 8 pre-selected GSM telephones, such as those of the blasting foreman and site supervisor. A measurement report from all measuring points, no matter how many there are, is ready within a few minutes of the round being fired and can be used to present the vibration results for each round individually, or for all rounds fired so far.

At the NCVIB portal, the contractor can enter each round into a digital blasting journal, including all information about charges, hole-depth, number of holes, and so on. Since the position of the round is marked on a cyber-map of the site, the round coordinates are obtained automatically. The maximum permissible vibration levels are then calculated by the system. In a so-called measurement value report, you can read off the percentage vibration level relative to the limit value for each measuring point, and quickly determine whether or not any changes need to be made in the next round.

In the map (see Fig. 2) it is possible to see both the active and the inactive measuring points that have been set up. It is possible to zoom and pan in the map. Information about the various measuring points and the rounds that have been entered is obtained by simply moving your mouse pointer over them on the map.

To dimension your rounds, you need to optimise the detonation sequence and exploit all detonator delay times maximally. To facilitate this, there is an important function in NCVIB that enables you to obtain the time history record from the measuring point and study it in an external program called UVSZ (which can be downloaded). Alongside (Fig. 3) is an example of a time history plot from one of the latest rounds blasted in the Törnskog tunnel. It was taken from the measuring point at No. 18 Kraftverksvägen, which was situated 66

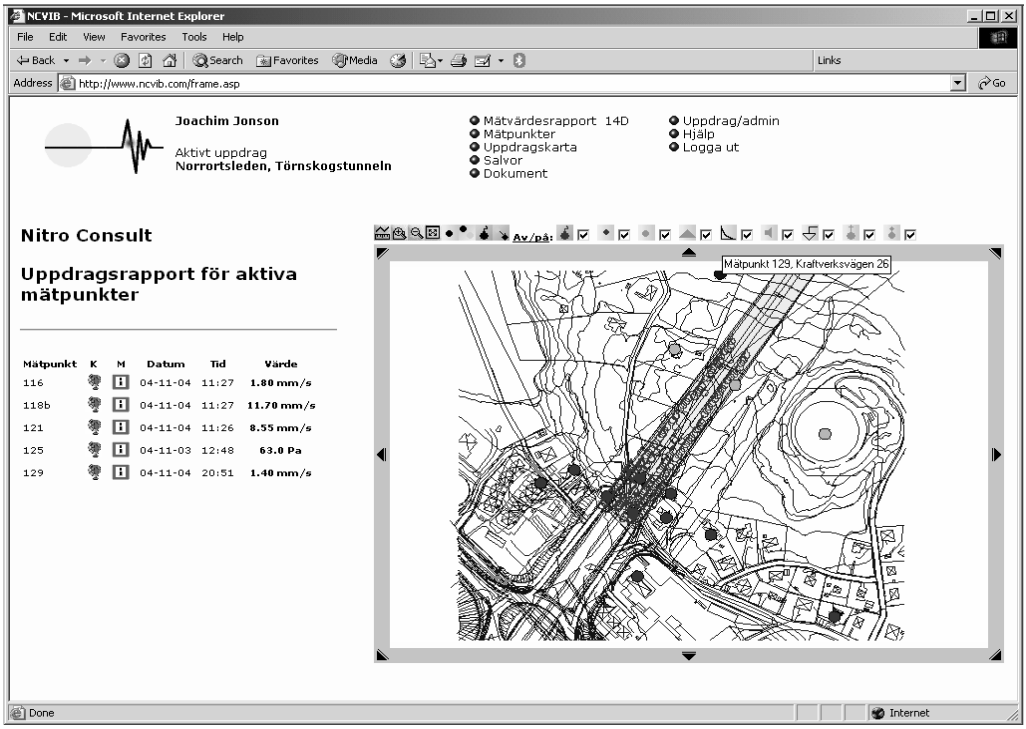

Figure 2. Map of the measuring points.

metres from the round. See also the measurement report (Fig. 4), which shows, for the same round, the velocity of vibration relative to the limit value at each measuring point.

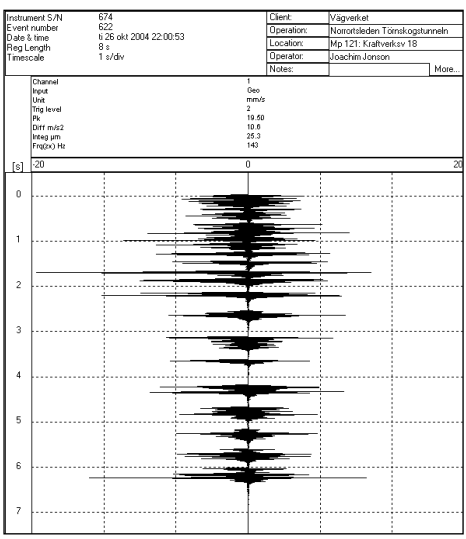

Figure 3. Round N44. Measuring point 121 at No. 18 Kraftverksvägen.

If there is a transmission fault for some reason – on the part of the telephone service provider for instance – so that contact between the measuring instrument and the data server is broken, there is no risk of losing the measurement data. The instrument has an internal memory capable of storing the measurement data for one month. If you wish to make copies for the sake of security, it is simply a matter of telephoning the instrument via UVS REMOTE and copying the memory of the instrument for the latest month.

3 TUNBERGET JUNCTION – CONTRACT 211:012

Contractor: Oden Anläggning AB

In September 2002, construction of the remaining parts of Norrortsleden started with preparatory works that included the rearrangement of utility service lines south of the proposed Törnskog tunnel. At the beginning of 2003, the contract for the Tunberget junction (Fig. 5) began with the down ramps to the Törnskog tunnel, which required approximately 20,000

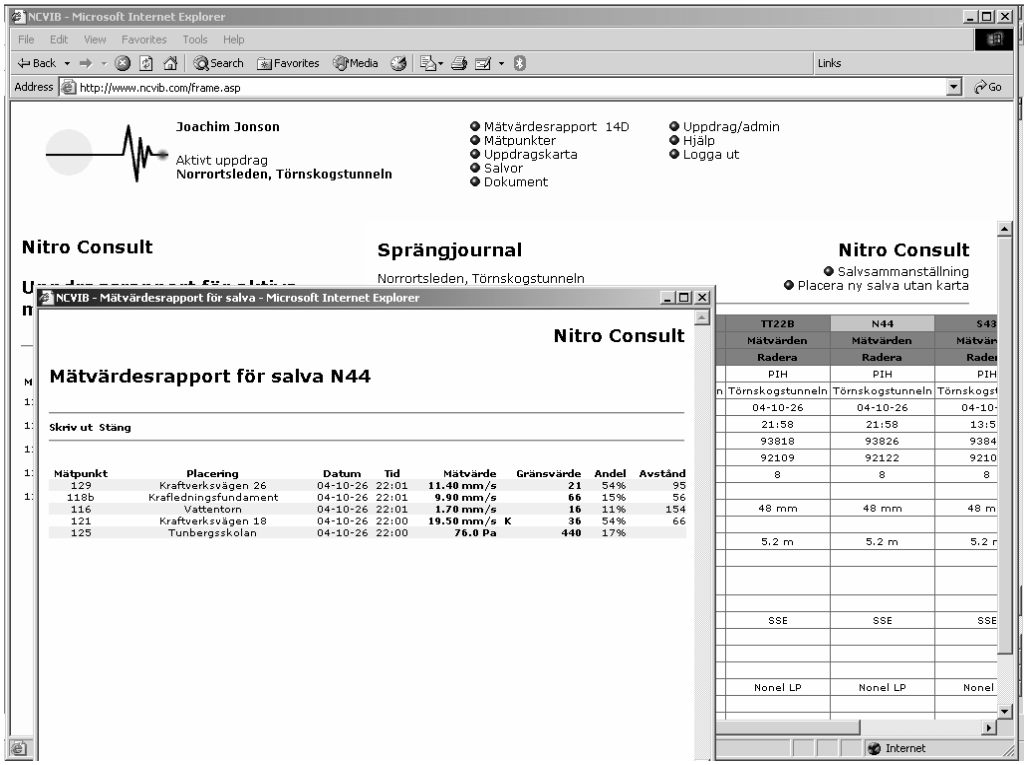

Figure 4. Measurement value report for round N44.

m^3 of rock to be excavated. In a supplement to the contract, the client ordered the driving of 2 x 110-metre lengths of motorway tunnel, i.e. the southern ends of the Törnskog tunnel, on which work began in December 2003.

Preparatory work for the Tunberget junction included the demolition of a few apartment blocks and the re-routing of a high-voltage power line, as well as some district heating pipes and the district water main, which was situated right over the area where the open cut for the tunnel was to be excavated.

Prior to the start of blasting, Nitro Consult carried out preliminary surveys of the buildings in the vicinity and pressure-tested various chimney-stacks.

Blasting for the open cut leading into the tunnels had to be carried out with consideration to buildings around the work site, as well as the power-line roads and the new water pipes. The distance to a raise-bored tunnel containing water pipes was about 10 metres. The distance to the nearest pylon foundation to the northeast of the excavation was also just 10 metres. The open cut is about 60 metres wide, ranges from zero to approximately 20 metres in depth and is excavated out of steeply sloping rock. The job was tackled by dividing the rock into two benches.

In addition to avoiding damage to surrounding buildings and other installations, the blasting consultants had to ensure there would be no damage to the crests of the prospective tunnel portals, caused by backbreaking and lifting of the rock.

The deepest holes in the contour of the open cut were about 14 metres, and in the rounds about 13 metres. The bench holes were drilled with a burden of 1.8 metres and a spacing of 2.5 metres. They were given 3 metres of stemming in order to minimize the risk of fly rock from the upper parts of the holes, which had a lighter burden due to the relatively steeply sloping surface of the rock.

The bottom charge in the bench holes consisted of one 50 ^{x} 560 mm tube of the Dyno Nobel NG-explosive, Dynomit®, followed by the bulk explosive Titan 7000, a site-mixed

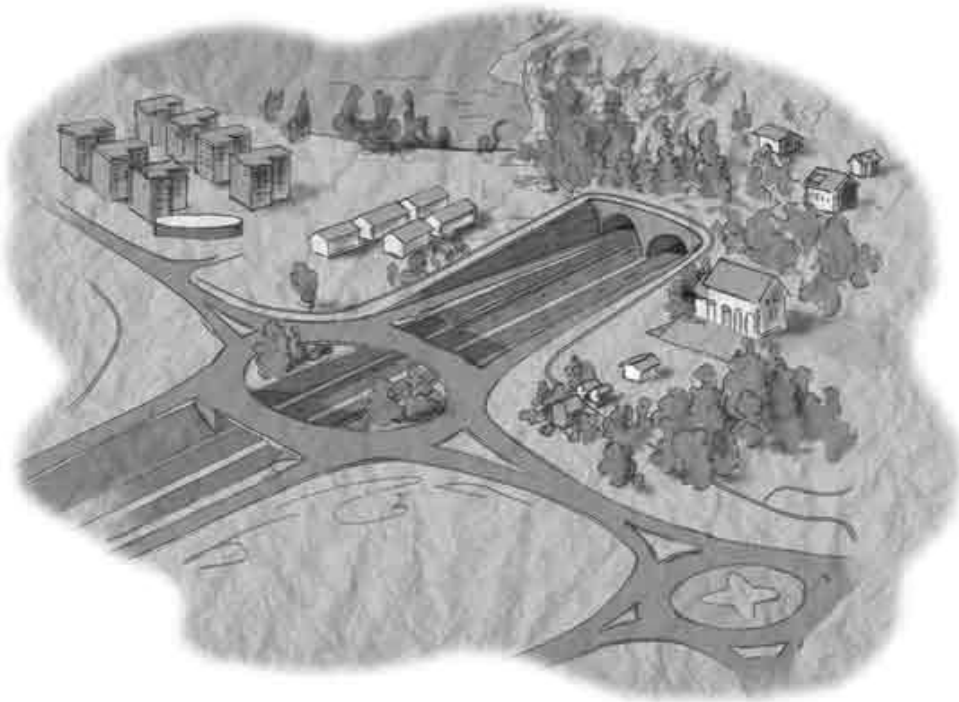

Figure 5. Tunberget junction with down ramps to Törnskog tunnel, as it will look on completion.

emulsion (SME) developed by Dyno Nobel. The helper holes were charged with one 29 x 1100 mm Kemix A plastic-pipe charge, which is a detonator-sensitive emulsion explosive made for Dyno Nobel by OY Forcit of Finland. The contour holes in the tunnel portals were bottom-charged with one 29 x 1100 mm Kemix A plastic-pipe charge followed by 40 g/m detonating cord. The contour holes in the side-walls were charged with 160 g/m detonating cord.

The biggest simultaneously detonating charge weight in the Ø 64-mm bench holes was 17 kg. Two deck charges were used in the bench holes.

The round consisted of about 400 holes, of which 250 were bench holes and 150 were contour holes. Roughly 7000 m^3 of rock was blasted by the round. In total, the round was charged with 4.2 tonnes of explosive, which gave a specific charge of around 0.6 kg/m^3.

Vibration was measured at 15 measuring points on buildings and installations in the inventory zone. Blasting of the big round went well, although an interruption in the initiation process in a later part of the round increased the load on the holes at the back of the round. This resulted in a sharp rise in the level of vibration, which can be seen in the time history record below (Fig. 6).

The limit value for the measuring point in Figure 6 was 35 mm/s for the distance in question. The highest velocity of vibration was 71.5 mm/s, and the displacement 0.17 mm. Other delay periods, except for three that exceeded the limit value marginally, gave vibration levels below the limit value.

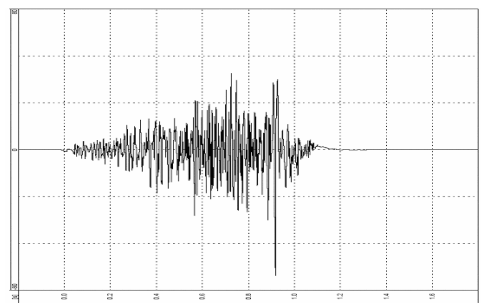

Figure 6. Time history record from measuring point on house at No. 12 Kraftverksvägen, situated about 45 metres from the round. The highest velocity of vibration was 71.5 mm/s, which occurred after 0.92 seconds.

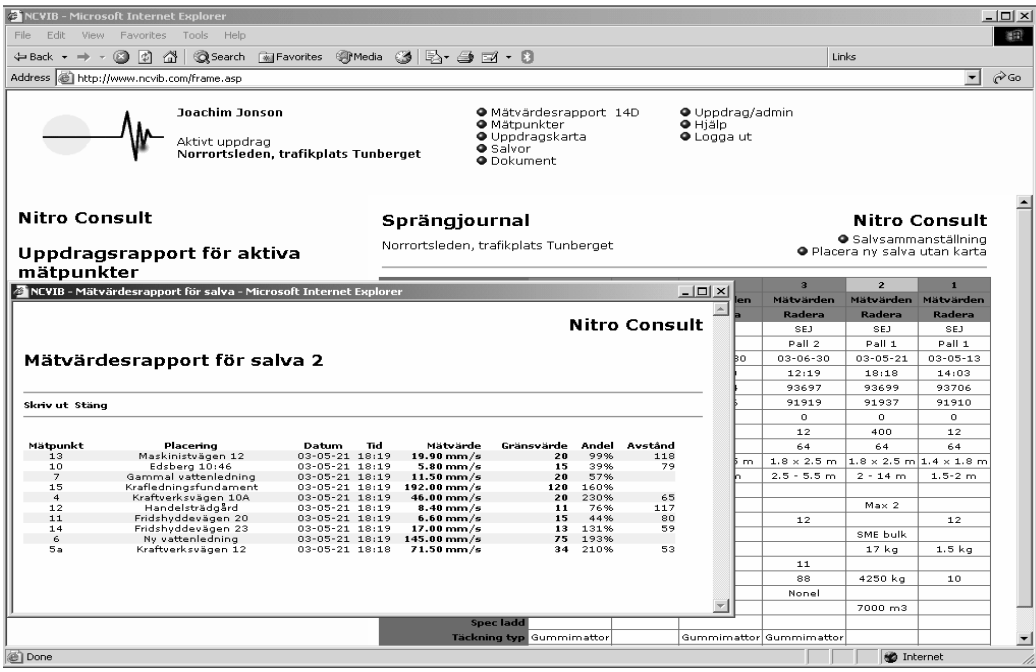

Figure 7. Measurement value report for round 2 at Tunberget junction, 21st May 2003.

The limit values were exceeded on the water pipe and pylon foundation as well. Above (Fig. 7) you can see the results from the nearest measuring points for this round, taken from the NCVIB portal.

Residents living in the immediate vicinity were forewarned about a week before blasting took place. In spite of this, a number of them were surprised by the blast. Complaints were made to Vägverket, although mostly by people who lived outside the immediate surroundings of the site. This was perhaps to be expected, for they were much too far away to hear the siren. Detonation of the Tunberget rounds could be compared to the blasts that take place in medium-size quarries, if one disregards the fact that deck loading was employed. The most distant complaint came from someone who lived nearly one kilometre from the work site. The vibration level at that distance is estimated to have been less than 1.5 mm/s, which is far below the guide values applicable to such distances.

Once the open cut had been excavated, drilling for the first legs of the double grout shields for the tunnels was able to commence.

The Törnskog twin motorway tunnels will have 3 lanes each in the first stage. For the first 100 metres, the tunnel height is about 10 metres and the width about 20 metres. The remaining parts of the tunnels have cross-sections of 92 and 102 m^2 respectively. The contractor began blasting the tunnels during week 4 of 2004.

3.1 Measurement of structure-born noise

Drilling for the tunnel grout shields started at Tunberget junction at the beginning of January 2004, prior to the start of tunnel blasting. Both tunnels are being given a double grout shield, 18 and 27 metres respectively in advance of the tunnel face. The distance between the bottoms of the grout holes is 2.5 metres. The distance to the tunnel contour from the inner grout shield is 4 metres and from the outer shield, 5 metres. A total of 2300 metres were drilled for the first leg of the double shield. The grout-hole diameter is 64 mm.

All drilling work has to be followed-up by measuring the structure-born noise in the buildings that are nearest to the tunnel, and therefore considered vulnerable to noise disturbance. Measurements are being taken primarily in buildings whose foundations rest directly on rock, but also in buildings in areas where there is little rock cover. In fact, measurements will be taken at any place where it is feared that the

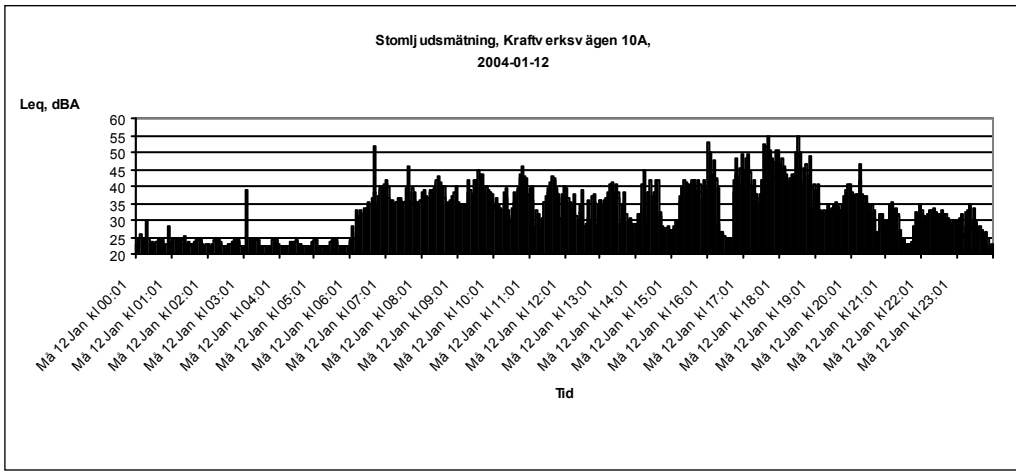

Figure 8. Measurement of structure-borne noise at No. 10A Kraftverksvägen, 12th January, 2004.

noise level might come close to the prescribed limit value.

During drilling for the first leg of the double grout shields, structure-borne noise measurements were taken in two buildings, one founded on rock, the other on moraine. The one whose foundations are in moraine is situated about 40 metres from the tunnel portals. The distance from the building to the nearest grout hole was about 15 metres. During initial measurements, the highest equivalent sound power level was 45-50 dBA, registered at a distance of 17 metres. The prescribed limits for equivalent sound power levels are 50 dBA during daytime (07:00 to 18:00 hrs), 40 dBA during the evenings (18:00 to 22:00 hrs) and 25 dBA at night.

It can be seen from the time history record (Fig. 8) that the drilling was done during the day. The quieter periods during the day indicate when the drill rig was being repositioned and set up for drilling. At some time between 16:00 and 17:00 hrs there is evidence of some kind of noise source, probably the residents of the building returning home from work and increasing the noise level.

4 TÖRNSKOG TUNNEL – CONTRACT 211:013

Contractor: Oden Anläggning AB

This contract is a continuation of contract 211:012, in which tunnel blasting started at the end of January 2004. It comprises 2 x 2 kilometres of parallel tunnels and about 700 metres of motorway. About 150 000 m^3 of rock was excavated in the open cuts at the north portals. About 460 000 m^3 of rock will be excavated in the tunnels themselves.

For about half of their distance, the tunnels will pass directly below the Törnskog residential district. They will be located between 10 and 20 metres below ground level. In three of the bigger depressions along the route of the tunnels, the rock cover falls to about 7 metres at the least. The overburden in such places varies between 3 and 9 metres in depth.

By the beginning of November 2004, the advance was about 230 metres from the south portals in both tunnels. The advance from the north portals at Norrsättra was about 55 metres. In the south, the contractor was approaching one of the most critical sections, Solängsvägen, which has the least rock cover, with houses situated directly above the tunnels.

Owing to restrictions on structure-borne noise, neither blast-hole drilling nor grout-hole drilling can be carried out at night while the tunnel faces are beneath the residential district. The prescribed limit values for structure-borne noise, airborne noise, vibration and airborne shock waves are given in the risk analysis.

Structure-borne noise and vibration are being measured continuously on buildings above and to the sides of the tunnel faces. The results of the measurements are being used to control the drilling and blasting schedules.

5 SUMMARY

The Nitro Consult system of instruments equipped with GSM modems and data

transmission, together with UVS REMOTE and the NCVIB Internet portal, makes it possible to read vibration, airborne shock waves and noise levels quickly and safely. It also enables all documents and blasting journals to be kept at the same place on the NCVIB Internet portal, which is accessible to any authorized person who is involved in the project and who can benefit from the information.

Reports and time history records showing the respective values for a round become available within a few minutes of the blast. This information can be used to plan and dimension subsequent blasts in order to optimise the round size and the advance, and to help contractors stay below the maximum permissible vibration levels.

REFERENCES

Karlsson, P.-O., Vägverket & Johansson S.-E. 2003. *Nitro Consult AB. Discourse BK 2003. Norrortsleden – A crosslink between the E4 and E18 – A blast-engineering challenge.*

SWECO VBB Viak & Tyréns AB. *Risk analysis, Norrortsleden, Edsberg – Täby Kyrkby section, 211:013 Törnskog tunnel.*

SWECO. Technical description of rock excavation for contract 211:01.

Brighton Conference Proceedings 2005, R. Holmberg et al

Experiences with a remotely controlled centralised blasting system at the Boliden Mineral Garpenberg underground mine

B.-O. Johansson
Boliden Mineral, Garpenberg Operations, Sweden

ABSTRACT: In Garpenberg, located in the Swedish county of Dalarna, Boliden operates two mines, the Garpenberg mine and the Garpenberg Norra mine. Mining is by cut and fill. In the Garpenberg Norra mine, where mining at present is taking place at the –1000 m level, many new technologies have been introduced which have contributed to an increased productivity and quality. These include a new mine map navigation, a drill plan generation system and a wireless centralised blasting system. This paper describes the remotely controlled centralised blasting system DynoRem Mine and the experiences we have had with the system for increased safety and productivity. The centralised blasting system is intended for remote initiation of up to 24 NONEL rounds below ground via radio control. The system consists of a PC, which is connected to a control unit, and up to 24 blasting machines can be connected to the system. These are controlled 'in groups" with 1–9 blasting machines in each group. The system has contributed greatly to increasing the safety in our mine.

1 INTRODUCTION

1.1 History

Boliden's mining operations in Sweden comprise three areas: Aitik, the Boliden area and the Garpenberg area. Boliden is also the owner of the Tara mine in Ireland.

Figure 1. The Garpenberg area.

The Garpenberg Mine is the oldest mine in operation in Sweden, and the mineral deposits were mined as early as in the thirteenth century. During the Middle Ages, mining operations were carried out by mountain dwellers, the Church and the Swedish government. Bishop Israel Erlandsson Ängel, who owned the copper mines in the early fourteenth century, retained German miners who were called 'garpar'.

This is the origin of the name 'Garpenberg'. One of the owners of the mines was Gustav Vasa, the first king of the Vasa dynasty. Boliden purchased the Garpenberg mine from AB Zinkgruvor in 1957. Operations at the Garpenberg Norra mine started in 1972.

1.2 Mining method

In the Garpenberg area a sulphide polymetallic ore is mined. Its main constituents are zinc and silver, but the ore also contains lead, copper and gold.

Mining is by cut and fill. Six metre slices are mined from stopes 50–300 m long and up to 15 m wide. The lowermost cut is filled with pure sand and later on with waste rock and sand; thereafter either plain or cemented tailings pumped from the surface are used and the water is drained off. The

coarse fraction of the mill tailings is used for backfill in the mines, while the fines are deposited in an adjacent tailing pond.

More than 1.1 Mt of ore is processed at the concentrator each year. The copper and lead concentrates are transported to the Rönnskär smelter, and the zinc concentrate to Kokkola Zinc, Norzink, and to external European smelters for metal production.

In 2003, production in the Garpenberg area corresponded to 80% of Sweden's zinc consumption, and to 50% of lead and 33% of silver production.

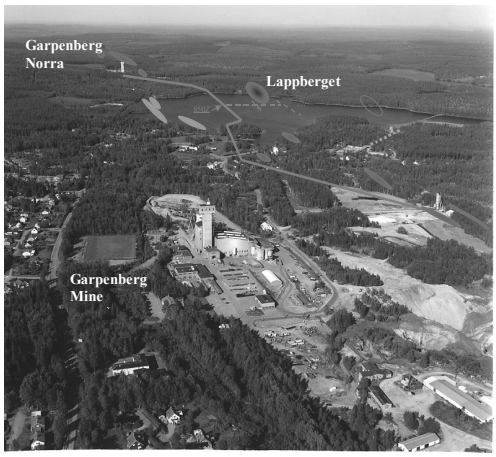

Figure 2. Aerial picture of the mining area.

The Garpenberg area is very interesting in terms of exploration. Between the two active mines, a large deposit, called Lappberget, was discovered in 2001, with high grades of zinc, silver and lead, extending the operating life of the area. This ore body is of a greater thickness then the Garpenberg mine and Garpenberg Norra mine ore bodies and will allow for a larger-scale mining method, i.e. panel stoping with paste fill. A connecting drift between the mines at 800–900 m level was completed in the spring of 2004, and production at Lappberget commenced on a wider scale.

The Garpenberg area has around 275 employees.

2 HEALTH, SAFETY AND ENVIRONMENT

2.1 HSE programs

Garpenberg Operations are continually focusing on health, safety and environment (HSE) in order to ensure a good working environment. In order to decrease risks of ill health or accidents, the working conditions are daily discussed at meetings at all levels.

Risks such as falling rocks in the mines are continually discussed and analysed. Cautious blasting, mechanised scaling and better methods of rock bolting are continually improved to reduce the risk of falling rock.

Safety courses and meetings are held to increase the employees' health and safety commitment. HSE campaigns are organised in order to focus on certain issues. Examples are fire protection and a recently performed project in cooperation with our explosive supplier in which we aimed to reduce the nitrogen emissions to water. We recently also conducted training for our employees and our contractors to increase environmental awareness. At the Garpenberg mines we have been successful in safety projects, and the LTIFR (Lost Time Injury Frequency) has been reduced considerably in recent years.

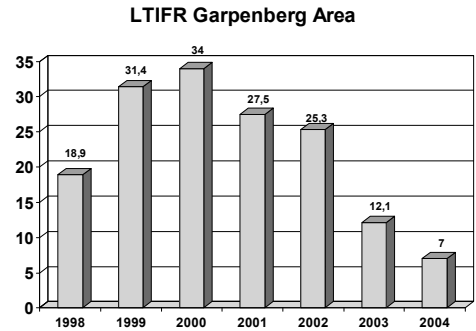

Figure 3. LTI per 10^6 hours.

2.2 Old blasting procedure

Blasting in the drifting and the production areas in an underground mine is a specific operation that is always of concern. At the Garpenberg mines we previously utilised a simple, but not the safest, method for initiation of the rounds.

In the mines the NONEL system is used, and, after charging the coupled rounds, we earlier had the blasting crew to drive around to the various blasting sites. At the end of each shift, i.e. at 16.00 and at 04.00, the crew ignited the Nonel rounds with cap and fuse. The new shifts started at 18.00 and 06.00, which gave us a time gap of 2 h to shoot the rounds and ventilate the blast fumes.

These operations were considered to be quite dangerous as we had people driving around between the various blasting sites in the mine for

initiation of the rounds. The old-fashioned cap and fuse were also not considered as safe as the NONEL system.

Dyno Nobel had for a few years leased out a central blasting system to the Portuguese mine Somincor, which caught our interest. After an analysis of the wireless equipment DynoRem Mine, we decided to install one in the mine for increased safety.

3 CENTRAL BLASTING SYSTEM

3.1 Mine communication system

The Garpenberg mines utilize leaky feeder as the mine communication system, and it was clear that this system could be utilised for the central blasting system. Leaky feeder is an effective system for two-way communication and data transfer. The frequency band is 460 MHz. Actually, the central blasting system DynoRem Mine transmits on 469 MHz and receives data on 459 MHz. As these frequencies cannot penetrate the rock, communication is primarily reliant on a cable system underground in the mines. This cable leaks the signal and makes it possible to allow for radio transmissions from and to the cable. Along the cable system a number of amplifiers are placed in order to ensure that a consistent signal level is maintained throughout the system.

3.2 DynoRem Mine

In 2003 the supplier Dyno Nobel visited us a few times for initial trials and adjustment of the system for reliable use. Figure 4 shows a sketch of the system and how it is used.

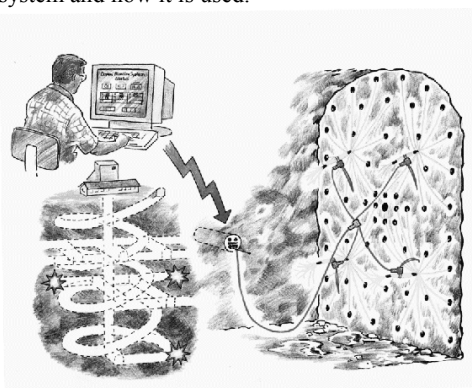

Figure 4. Principle of the central blasting system.

The central firing system is intended for remote initiation of up to 24 Nonel rounds below ground via radio control. The system consists of a personal computer (IBM PC compatible), which is connected to a control unit, and 1–24 blasting machines can be connected to the system. These are controlled 'in groups' with 1–9 blasting machines in each group.

3.2.1 Control room

Adjacent to the shaft at the 800 m level, a control room for the central blasting system was established.

The PC in the control room works partly as a tool for designing the blasting system and for grouping and setting the so-called blasting timeframes, and partly as a communication centre with code transmitters.

An access code is required for the use of the control program in the computer.

The access codes can be granted on two levels. The lower level authorises blasting and other system functions except for the setting of blasting timeframes and the input of access codes. The higher level gives access to all system functions.

Figure 5. PC in the control room.

Figure 6. Control unit.

The control unit includes a radio modem, a computer card and charging/firing command keys, and it can be protected against unauthorized use with the help of a key switch.

3.2.2 Blasting machines

For the central firing system there are two varieties of NONEL blasting machine. One has a cylindrical shape of 9 cm diameter and 42 cm length. A rechargeable battery, which is attached to a bayonet fitting at the back of the casing, powers the machine. The other is in the shape of a box measuring 30 × 20 × 8 cm. It has a built-in battery, which can be recharged via a connector on the machine panel. The cylindrical model machine is fitted with a strap to carry it, and the box machine has two handles on the panel.

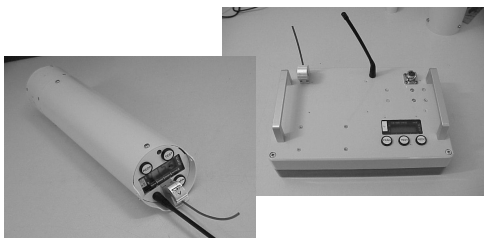

Figure 7. Blasting machines.

The cylindrical machine was designed so it would be easy to protect it from debris coming from the round. It was supposed to be placed in a Ø102 mm drilled hole placed at the wall of a drift. However, it was not very convenient to drill that size hole as we were not using the drill diameter in our development or stock blasts. Therefore, we just make sure that the blasting machine is placed at a safe distance from the round itself.

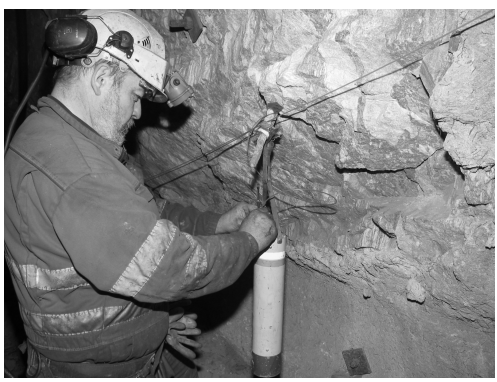

Figure 8. Preparing the cylindrical blasting machine for a blast.

The blasting machines contain a spark igniter for the firing of a NONEL tube, a code receiver with a real-time clock, and an individual fixed and unique ID code, as well as a communication radio.

The tube holder with the spark electrode, which is found on the blasting machine panel, senses and registers if there is a NONEL tube in the holder. On the panel there is also a radio antenna.

The blasting machine panel has a display that shows the actual time, and at the side of the display there is an ID code of the machine. Around the display there are LEDs that show the different statuses of the blasting machine. The machine is supplied with power from a rechargeable battery, which provides an operation period of at least 22 h.

4 BLASTING

When we prepare for the blasting at the end of each shift, i.e. 16.00 and 04.00, we follow a simple scheme.

Making ready for blasting should not be carried out more than 22 h before the intended firing time as the blasting machine battery cannot be guaranteed to keep the machine activated longer than that.

The blasting crew place the blasting machine in a well-protected place away from the round.

We connect a piece of empty NONEL tube to the spark electrode and make a connection test. If we do not find any position where connection can be reached, the blasting machine has to be moved to a different spot.

The blaster connects the lead in line from the NONEL blast to the blasting machine and makes a final test to assure that the 'Ready' LED on the panel comes on. Even if the central blasting system is in a blasting timeframe, the blasting machine cannot for safety reasons be activated for another 15 min after the 'Ready' LED has come on.

After the blasting crew has prepared all the blasting machines, they return to the control room and our routine ensures that there are no miners or maintenance people elsewhere underground.

In the control room the operator uses the access code to gain control over the central blasting machine and the necessary timeframes for each individual blast. The control unit is easy to use, and, after testing that the communication is clear to all blasting machines and it has been confirmed that the NONEL tube is still attached to the

blasting machine, the operator is ready to fire the blasts.

If the blasting timeframes are changed in the control unit after the blasting machine has been activated, the change will not go through to the blasting machine. For the change to be registered in the machine it has to be switched off and then re-activated.

The operator can group the blasting machines to be used, and, after he presses the FIRE button, the control unit takes over and fires each blast at the predetermined interval time. However, we prefer the operator to press the FIRE button for each individual blasting machine as this saves us some programming time.

The operator receives confirmation that each individual blasting machine has fired, and he will also receive confirmation that each blast has gone off through a microphone at each of the blasting machines.

After the blasts, the operator shuts down the central blasting system.

When returning to the blasting site after blasting, the blasting machines are to be turned off and taken to the control room for recharging of the batteries.

5 CONCLUSIONS

The system has been working excellently after initial trimming at the mine site. When we used cap and fuse to initiate the rounds there was a safety concern as the vehicle used by the blasting crew to drive from blast site to blast site could break down, causing risks of exposure to detonation fumes from blasted rounds. Avoiding the need for people to enter the mine during the initiation sequences is a safer approach than the method previously used. A central blasting system like DynoRem Mine is convenient to use, and safety has been increased in the mine.

Brighton Conference Proceedings 2005, R. Holmberg et al

Advanced automatic optical blast fragmentation sizing and tracking

T.W. Palangio & T.C. Palangio

WipWare Inc, Bonfield Ontario, Canada

N. Maerz

University of Missouri-Roll, Rolla, MO, USA, and WipWare Inc, Bonfield Ontario, Canada

ABSTRACT: Sizing of blast fragmentation using digital image analysis has proven an effective way to evaluate the results of blasting technique. Image analysis methods like WipWares's WipFrag system work best under controlled conditions like over moving conveyor belts, where camera angles and distances can be held constant, lighting can be controlled, and sampling errors can be kept to a minimum. However, once the fragmentation is on the belt, it has usually passed through a primary crusher and is no longer completely indicative of the blasting process. In practice, for many operations, this means that the best measurements can be made by imaging the rock while in transit between the muck pile and the primary crushing station. This includes surface and underground HD (Haul Dump) and LHD (Load Haul Dump) type vehicles which can be images as they dump, or prepare to dump, or as they pass through a gate or other restriction.

1 INTRODUCTION

1.1 Optical sizing

Size distribution is a critical component of managing any mining operation, from the drilling and blasting to the final product; the material size dictates all downstream operating costs.

Previously, the only way to measure a size distribution was to stop production, manually collect a sample, pass the sample through a battery of screens, weigh the material on each screen and plot the data on a granulation curve to reflect what size the material was at the time of sampling. This method is slow, cumbersome, disruptive and impractical for the sizing of blasted material where the particles can range in size from microns to meters. Even though sieve analysis offers a high degree of precision and accuracy within the sample, the sample size is traditionally very small, making the results much less representative.

In 1987 the WipFrag photoanalysis system was developed to characterize the size distribution of blasted material. This system was the first of its kind of optical sizing system, and offered significant advantages over preceding methods such as speed and ease of use. It was non-disruptive and practical for sizing any material that could be successfully imaged, including blasted material.

Since then, photoanalysis has been used in a number of applications around the world, such as the analysis of muck piles, conveyor belts, surge bins and, most recently, vehicle conveyances. This technical paper describes the evolution of this technology into case-specific applications of automated vehicle conveyance analysis.

1.2 Muck pile analysis

Automated sizing analysis of muck piles has been done for many years (Fig. 1). A review is given by Franklin et al. (1996). The WipFrag System first proposed in 1987 (Maerz et al. 1987) and commercialized in 1996 (Maerz et al., 1996), was initially used primarily to characterize the size distribution of muck piles. Various studies attest to the success of this approach (Bartley and Trousselle 1998; Chiappetta 1998, Ethier et al. 1999; Barkley and Carter 1999; Palangio and Maerz 1999).

Still, muck piles are inhomogeneous, natural lighting conditions vary, depending on sun angle

and cloud cover, and camera angles can be quite variable. These and other errors were studied and quantified (Maerz and Zhou, 1999); Maerz and Zhou, 2001). From these studies the following factors were identified as most important in improving the accuracy of the measurements:

- consistent image quality, including uniform and constant lighting;
- fixed scale of observation;
- elimination of sampling biases.

Although consistent image quality, lighting, and camera position can be maintained with careful effort; the possibility of eliminating serious sampling biases when measuring muck piles is not great.

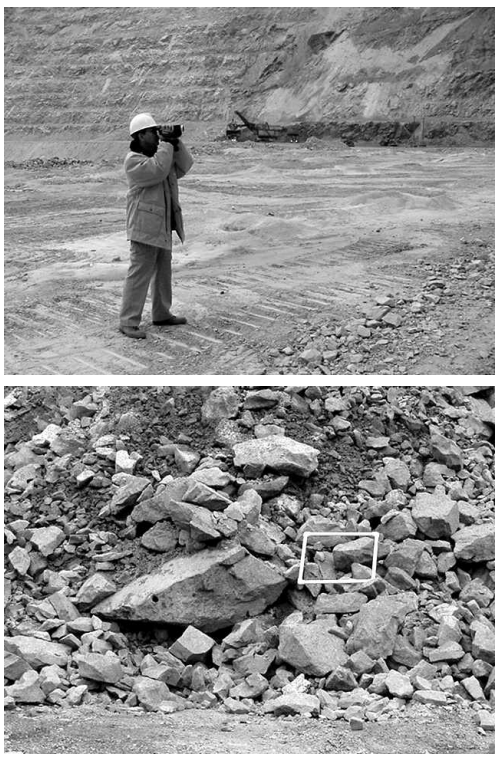

Figure 1. Image of a muck pile (bottom) taken with a roving camcorder (top); there is a scaling device in the foreground of the image.

1.3. Conveyor belt analysis

Measurements made on conveyor belts (Fig. 2), by their very nature solve most of the above problems. Consistent image quality can be ensured by providing artificial lighting in a controlled environment. Constant scale of observation is guaranteed by fixed mounted cameras. Sampling bias are severely reduced because a) all the material is sequentially paraded before the camera, and b) gravity segregation can be assumed to be constant and calibrated out. Various studies attest to the success of this approach (Elliot et al. 1999; Bouajila et al. 2000; Dance 2001; Maerz 2001).

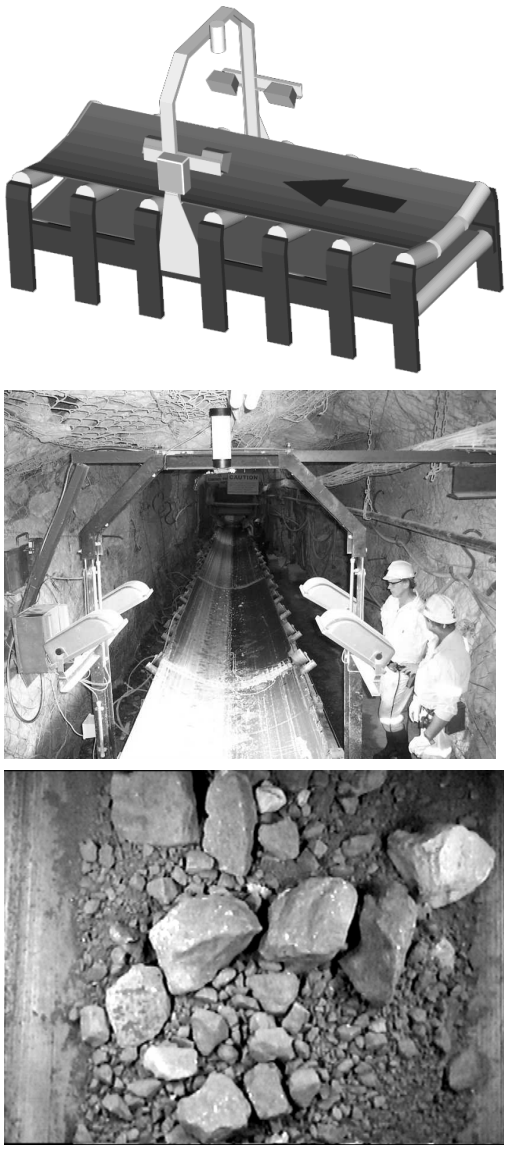

Figure 2. Imaging set-up of camera and lights (top and middle). Image of fragmentation on a conveyor belt taken with a fixed camera and fixed lighting mounted over a conveyer belt (bottom).

The difficulty in conveyor belt applications is that the blast size distribution has already been altered by primary crushing, since in most cases the conveyor systems begin only after the primary crusher.

1.4 Primary crusher feed bin analysis

The surge bin to primary crusher (Fig. 3) set-up makes a reasonably good analysis point, the material is representative of the blasting, only minor degradation of the material has occurred due to loading, haulage, and dumping. This method also allows for moderate control over other variables such as lighting, scale and environment.

There are several difficulties with this approach. These configurations are very uncommon in the industry and are highly prone to jamming, which will introduce a unique error since the system will image the same material multiple times, biasing the sample. In addition, much of the time the bin sits empty or there is not enough material in the bin to do a proper analysis. This also introduces errors into the system.

Figure 3. Fragmentation in primary feed bin.

5.1 Truck conveyance analysis

The best option, therefore, for automated analysis of blast fragmentation is to image and analyse the fragmented material in transit between the muck pile and crusher in the conveyance vehicles (Fig. 4). This implies both surface and underground haul dump (HD) and load haul dump (LHD) type vehicles.

2 TRUCK CONVEYANCE MONITORING

2.1 Introduction

Hundreds of case studies and years of data validate the WipFrag engine used to determine the size distribution of material in images; therefore there was no question whether or not the material could be successfully analysed in vehicles, since this has been done manually for years. The real challenge was the design of an intelligent fragmentation analysis system capable of waiting for minutes, hours, or days for the presence of specific samples.

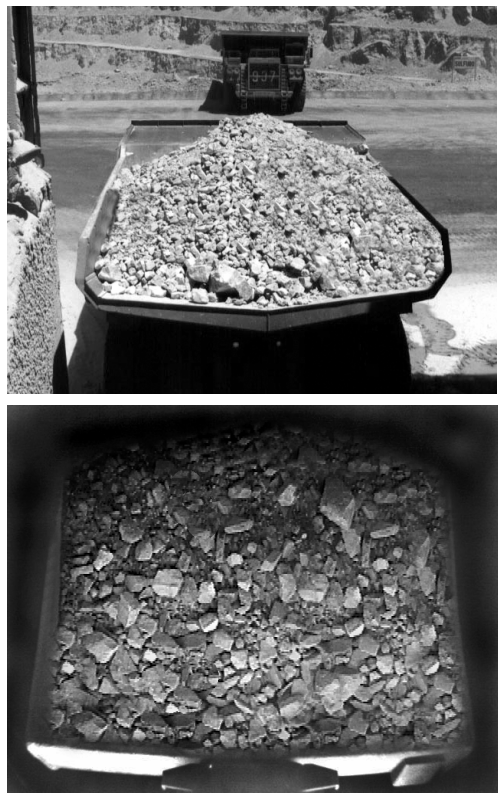

Figure 4. Image of fragmentation in back of truck (top) and in bucket of load haul (LH) vehicle (bottom).

In 2001 WipWare developed a system specifically for this purpose: WipFrag Reflex. By the final stage of development the system would exhibit near-human qualities as it would need to execute many complex functions in order to obtain a suitable image for analysis such as:

- 'sense' the presence of a sample;
- 'wake up' from a dormant state;
- 'identify' the vehicle and origin of material;
- 'determine' whether or not the bucket is full or empty;
- 'image' the bucket;

– ‘discard’ any parts of the image that do not show rock material;
– ‘analyse’ the image with an advanced fragmentation analysis system;
– ‘collect’ the information in a comprehensive database;
– ‘share’ the information over a network;
– ‘sleep’ if no further activity is detected.

These complex functions would require significant expansion of sensory capabilities, breakthrough development of system logic and the tight integration of tracking technology with analysis results.

2.2 Triggering system

On conveyor belts with a continuous stream of material, timing of the imaging process can be left up to the software. When the software is ready for the next image, it can trigger an acquisition, knowing that any image it takes should be adequate. The condition of empty or stopped belts can be signalled to the software using transistor–transistor logic (TTL) signals, or using OLE for process control (OPC).

For imaging material in individual vehicles, no longer can the software sample on its own time; an advanced triggering system needs to be integrated into this system, which would be responsible for multiple aspects of the image acquisition process.

Ultrasonic (Fig. 5), microwave, and optical recognition type triggering have been integrated in the system. Ultrasonic triggering offers good range, is waterproof, robust and reliable even in harsh environments, is safe and triggers consistently. Microwave triggering is very good in extremely dusty environments. Mechanical and pressure triggering was ruled out as a reliable triggering system, as large and heavy vehicles would be likely to damage small, delicate contact-type triggering devices. Laser and IR beam triggers proved to be oversensitive causing false triggers due to dust particles and other foreign obstructions. Radar worked well but was very expensive and posed health concerns.

Optical recognition triggering is used as a secondary triggering device; it utilizes the existing camera infrastructure by capturing multiple images and comparing them to each other, triggering only when a difference is detected over a given range of pixels (picture elements). Optical recognition triggering on its own is normally not adequate.

The tracking system (section 2.3) can also be part of the triggering process, as it can be used to determine the proximity of the target vehicle.

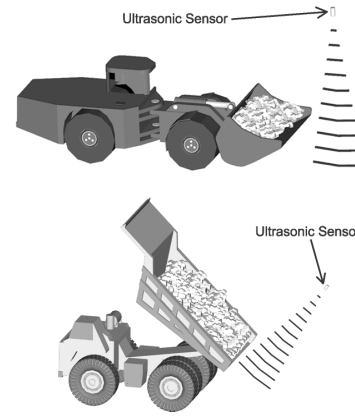

Figure 5. Use of ultrasonic sensors to determine the presence of material, either being transported (top) or dumped (bottom).

2.3 Tracking system

In a typical mining application, rock is transported from different parts of the mine, different rock faces or separate blast areas. Consequently the source of each truckload needs to be recorded to allow the system to merge the appropriate information.

There are several types of tracking system that will lend themselves to this criterion such as global positioning system (GPS); differential global positioning (DGPS), active radio frequency identification (RFID), passive RFID, line scanning (bar codes) and optical character recognition. GPS and DGPS were ruled out owing to high cost, difficulty of integration, inability to determine exactly which vehicle is currently dumping at a crusher (in the scenario of multiple access crushers, because of limited resolution), inability to carry programmed information bits and suitability only for surface applications. Combined with previously collected field data, line scanning and character recognition were ruled out as a reliable method of tracking vehicles as it would require continuous processor usage, and would be subject to numerous read errors from dirty or obstructed bar or character codes on the vehicle. Passive RFID was initially very promising, meeting most of the required criteria; however, limited write capabilities with poor read/write

speed and low range (0.5 m or less) ruled out this method of tracking vehicles.

An active RFID type tracking system was chosen to be integrated into the WipFrag Reflex System. Active RFID tracking systems offer excellent range (15 m), low power consumption, and high speed consistent read/write performance that is both robust and reliable, even in harsh environments. In addition, the tag can dynamically store data, such as the weight or source of the material.

A single active RFID tag reader/writer is located in close proximity to the camera unit and lighting, and an optional tag writer can be put in

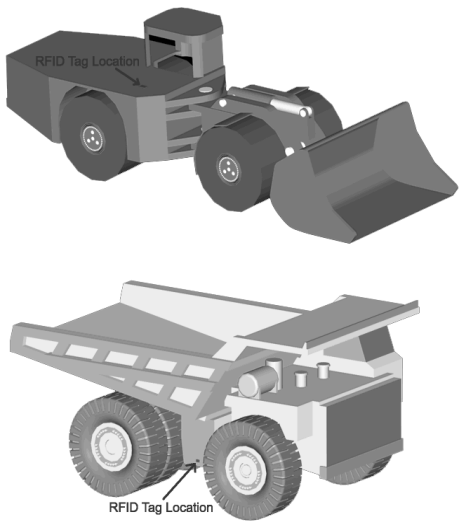

Figure 6. RFID Tags on vehicles.

the area where mucking is taking place, to identify the source of the material. On the truck is a tag (Fig. 6) which has a long battery life (10 years), low maintenance, is reasonably priced, hermetically sealed, resistant to oil water dust and impact, easy to mount, has the ability to work in proximity to magnetic ore types and be capable of being mounted directly to metal without seriously reducing the effective range.

The tagging system also complements the triggering system. Since the tagging system can only identify a truck within a range of a few meters, it can override false triggers when a valid truck is not present. This will reduce the chances of triggering on, for example, service vehicles.

2.4 Vehicle positioning

On a conveyer belt, the rock to be measured is always at the same place with respect to the camera. For muck pile sampling, image positioning is done by an operator. However when measuring rock in moving images (in an automated system) a problem that comes up is that the vehicle is not always in the same position. Consequently there is a possibility that any given image is not centered over the vehicle, which will result in erroneous measurements.

The solution is to capture the image as the vehicle always passes a fixed point, or alternatively force the vehicle to drive into that position (Fig. 7). In the case of truck tipping, a good location is the tipping station, since the truck is typically in the same position, and it is not moving at that point. For underground haulage, a good location is in narrow passes where the conveyance vehicle is naturally channelled into a narrow lane.

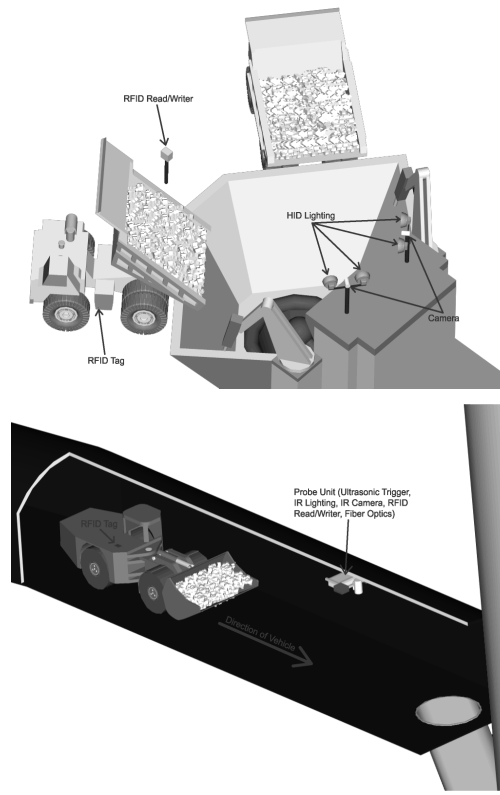

Figure 7. Camera, lighting, and RFID tag reader set-up in a position to force trucks into the correct position to be imaged.

2.5 Image limit detection

An intelligent image exclusion zone feature (a way of distinguishing between rock, and objects such

as the edges of the container) was required to ensure that only the rock material in the bucket or truck bed part of the image is analysed instead of other items such as the vehicle, ground or background. This is because the edge detection algorithm will attempt to force edges onto everything on the image, including those of foreign materials.

2.6 Lighting systems

On conveyor belts, adequate lighting is not difficult to attain, since a relatively small area from a relatively small standoff distance needs to be illuminated. However, when even illumination must be provided to negate sunlight effects on vehicles larger than a house under both day and night conditions or illumination of large conveyances in a pitch black underground environment, other concerns arise, such as lighting fixture cost, cost of maintenance, cost of operating and safety.

HID type sodium and HID type metal halide provide the best solution for surface applications, even though the lighting has a moderate initial cost, there are numerous advantages – such as moderate operating cost, reasonably high efficient, resistance to vibration, long bulb life – and are generally well suited for outdoor industrial heavy duty environments. The average bulb life of a HID metal halide bulb is 13000 hours, and the colour temperature is similar to daylight, making it more desirable. Both lighting types generate some heat but it is not excessive.

LED array visible and infrared type lighting is the best solution for underground applications owing to its extremely low power factor and resistance to environmental factors such as moisture, vibration, shock (concussion from blasting), dust and temperature conditions, coupled with the longest average bulb life of all lighting types – 60,000 hours (over six years of continuous use). LED type arrays are very light and have built in redundancy against lighting failure (if one LED burns out, then there are a few thousand left). The disadvantages to this type of lighting are initial cost, as these lighting types are somewhat expensive, though not as expensive as intrinsically safe fluorescent lighting, and the relatively low lumen output compared to other lighting types. The visible LED lighting may be disruptive to the vehicle operator (as would any type of lighting); therefore, infrared sensitive cameras combined with the infrared type LED lighting are used. The infrared LED illuminator is low powered and considered no more dangerous to personnel than a couple of 100 W lightbulbs. Another property that the infrared type lighting has over the other types is its ability to cut through dust particles suspended in the air; infrared light tends to illuminate the subject instead of illuminating the dust particulate, making this lighting type the best for the underground application.

2.7 Environmental Conditions

Dust, fog, rain, snow and particulates can be an issue if they obstruct the image or the triggering mechanism. Infrared lighting in underground applications will eliminate much of the dust problem; however, surface applications usually have more difficulty with this issue. WipFrag is equipped with software image filters that require certain image quality criteria to be met, prior to image analysis; this filter will discard any non-suitable images from a ‘set’ taken from a tipping event, for example when an HD type vehicle approaches the crusher to dump, the system will take a preset number of images (usually 3–5) during the dumping process; prior to analysis it will audit each image to determine if the image characteristics are suitable for analysis. If it is, the image is analysed; if it is not, the image is discarded.

Variable daylight conditions serve to confuse the image analysis sequence. Light intensity variations, sun angles, superstructure shadows, and differences between natural and artificial lighting all serve to create small differences in the analysis results. Solutions range from shielding the material from direct sunlight or operating at night only to accepting the errors.

In some occasions where a rock breaker is used, it may obstruct the camera view; this cannot be helped, and every effort must be made to position the camera to minimize this issue.

3 HD APPLICATIONS

HD applications are typically used in surface mining.

The Hamersly iron ore open pit mine in Australia is looking to reduce the number of fines and is verifying this using optical analysis on tipping trucks (Fig. 8). Two powerful quartz halogen lamps are used, one beside the camera mount, another from the side at an oblique angle. Imaging can only be done at night, as there is no shielding in place for direct sunlight.

Because of the fines, there is a tremendous amount of dust, a microwave trigger is used. The microwave beam is interrupted by the falling dumped rock, and sampling begins. In all, five images are taken at 2 s intervals, and then all images are analysed. (After 10 s of dumping, the images are generally too dusty to be useful).

Vehicle tracking is handled by the mine system using GPS, matching the truck movement with the timestamp provided by WipFrag.

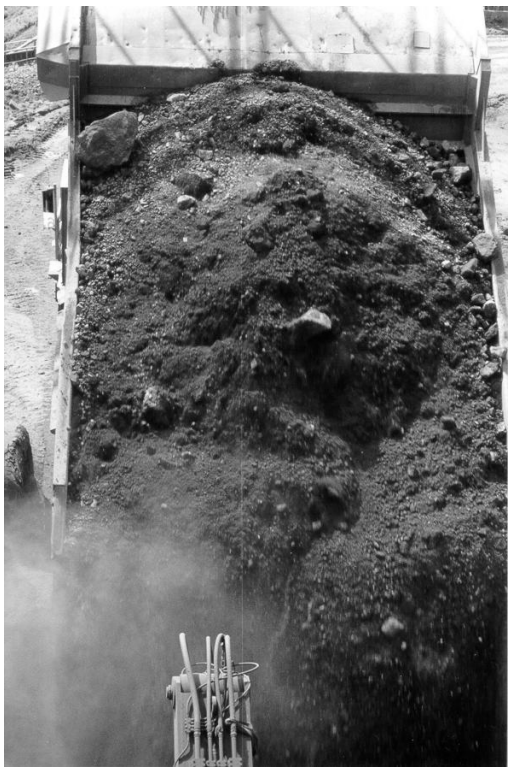

Figure 8. Truck Tipping at Hamersley Iron Ore, Australia; Early stage of dumping.

At the Caluahusi open-pit copper mine in Chile, they are looking to track blast results for their mine-to-mill optimization study (Fig. 9).

Two powerful HID metal halide flood lamps are used for each of the two dumping positions at the primary crusher; a lamp is located to the left and to the right of each camera. The system operates 24 hours a day, mainly owing to the predictable weather in the mountains; however, dynamic lighting conditions make night time analysis the most reliable, since there is no shielding in place to block direct sunlight.

Because of the lack of moisture, there is a significant amount of airborne dust during dumping. A laser trigger was initially implemented but has been upgraded since to a microwave triggering device that senses the presence of the vehicle commencing the sampling process. A cluster of five images are taken at 1.5 s intervals and are later analysed and merged after the vehicle leaves the dump position.

Figure 9. Truck tipping at Caluahusi, Chile.

4 LHD APPLICATIONS

LHD applications are typically used in surface mining.

The INCO research mine in Canada (Fig. 10) does not produce any minerals; its sole purpose is to test new technologies in a massive sulphide mine environment where controlled studies can be conducted prior to releasing new technologies.

Underground configurations are safety oriented with two infrared light sources located on either side of the infrared camera so as not to blind the equipment operator. The integrated RFID tag reader/writer communicates data to and from the passing scoop tram; this information may include bucket full/empty, tag health, signal strength, battery levels, origin of material, and other useful production data, including timestamp for each bucket dumped at the ore pass. The system operates 24 hours a day; dynamic lighting is not an issue since the unit is located underground.

Dust and dirt obstruction is not a problem because infrared light has special properties regarding airborne particles, and an optional ultrasonic trigger is used.

One to three images are taken at 0.2 s intervals which are later analysed and merged after the vehicle leaves the dump position. Intelligent exclusion zones and filters discard images or analysis results that are unacceptable.

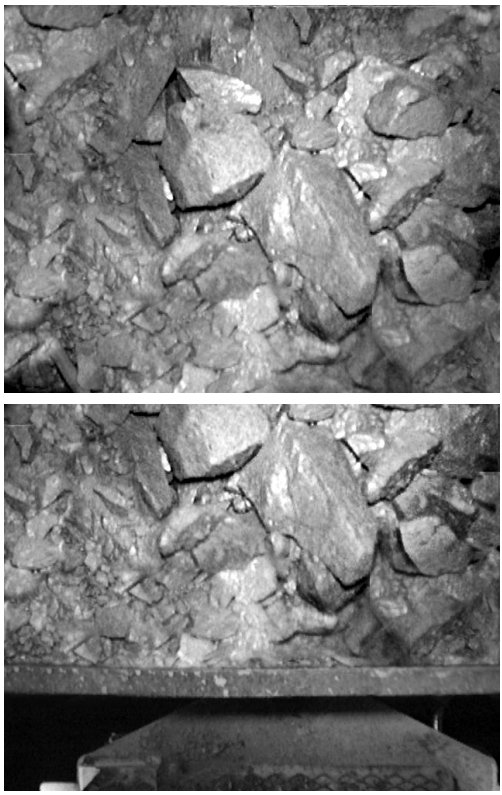

Figure 10. Sequence of images at INCO. Top: well-timed image. Bottom: image taken too late.

The LKAB Kiruna mine in Sweden (Fig. 11) is an underground iron ore mine, the largest of its kind in the world. They are looking to quantify underground blast results as well as track both manned and unmanned mine machinery, this data is used for mine-to-mill optimization studies.

Underground configurations are safety oriented with two infrared light sources located on either side of the infrared camera to not blind the equipment operator. The integrated RFID tag reader/writer communicated data to and from the passing scoop tram. The system operates 24 hours a day.

One to three images are taken at 0.2 s intervals which are later analysed and merged after the vehicle leaves the dump position. Intelligent exclusion zones and filters discard images or analysis results that are unacceptable.

Vehicle tracking is used; RFID tags are placed on each scoop tram located in a safe position close to the front of the vehicle. The RFID tags are relatively inexpensive and are considered consumable and disposable items if damaged or if the battery dies.

Figure 11. Tracking Ore at LKAB Mine.

5 CONCLUSIONS

Recent experience has shown that with technological innovations, the size of blast fragmentation can be measured where it is most useful, in transit on haul trucks, after being removed from the muck pile, and before entering the primary crusher.

This required adapting optical image analysis programs to act on external triggering, developing a mechanism to provide that trigger, and developing a way to force the truck into the correct position for imaging without disrupting the routine of the truck or truck driver.

In addition, because mining is typically a complex operation, with simultaneous muck from various source areas, vehicle tracking is required, to tie each measurement to the appropriate database.

Other issues include lighting concerns and issues of automatic rejection of poor images because of obscurement by dust (because no manual intervention is possible).

The cited case studies show that the methods described here are working and in use in a number of facilities, and are being used to measure the optimization of the blasting process for each facility.

REFERENCES

Barkley, T. & Carter, R., 1999. Evaluation of Optical Sizing Methods. *Proc. 25th Ann. Conf. On Explo-*

sives and Blasting Technique, Nashville, Tennessee, USA, pp. 305–324.

Bartley, D.A. & Trousselle, R., 1998. Daveytronic, digital detonator testing in a vibration sensitive environment. *Proc. 24th Ann. Conf. On Explosives and Blasting Technique*, New Orleans, Louisiana, USA, pp. 247–261.

Bouajila, A., Bartolacci, G., Koch, N., Cayouette, J. & Cote C., 2000. Toward the improvement of primary grinding productivity and energy investigation consumption efficiency. *Mine to Mill 2000*, Finland.

Chiappetta, R.F., Treleaven, T. & Smith, J.D., 1998. History and expansion of the Panama Canal. *Proc. 24th Ann. Conf. On Explosives and Blasting Technique*, New Orleans, Louisianna, USA, pp. 1–34.

Dance, A., 2001. The importance of primary crushing in mill feed size optimization. *SAG 2001*.

Elliott, R., Ethier, R. & Levaque, J. 1999. Lafarge Exshaw finer fragmentation study. *Proc. 25th Ann. Conf. On Explosives and Blasting Technique,* Nashville, Tennessee, USA, Vol. II, pp. 333–354.

Ethier, R., Levaque, J.-G. & Wilson, M. 1999. Achieving finer fragmentation and proving the cost benefits. *Fragblast 1999*. Johannesburg, South Africa, Institute of Mining and Metallurgy, pp. 99–102.

Franklin, J.A., Kemeny, J.M. & Girdner, K.K. 1996. Evolution of measuring systems: a review. Franklin, J.A, and Katsabanis, T. (eds). *Proceedings of the FRAGBLAST 5 Workshop on Measurement of Blast Fragmentation,* Montreal, Quebec, Canada. Rotterdam: A.A. Balkema, 1996, pp. 47–52.

Maerz, N.H. 1999. Online fragmentation analysis: achievements in the mining industry. *Center For Aggregates Research (ICAR) Seventh Annual Symposium Proceedings*, Austin Texas, 19–21April, pp. C1–1–1 to B1–1–10.

Maerz, N.H., 2001. Automated online optical sizing analysis. *SAG 2001 Conference Proceedings*, 29 September–3 October, Vancouver, Canada, pp. II250–269.

Maerz, N.H., Franklin, J.A. & Coursen, D.L. 1987. Fragmentation measurement for experimental blasting in Virginia. *S.E.E., Proc. 3rd. Mini-Symposium on Explosives and Blasting Research,* pp. 56–70.

Maerz, N.H., Palangio, T.C. & Franklin, J.A., 1996. WipFrag image based granulometry system. Franklin, J.A, & Katsabanis, T. (eds). *Proceedings of the FRAGBLAST 5 Workshop on Measurement of Blast Fragmentation, Montreal, Quebec, Canada.* Rotterdam: A.A. Balkema, pp. 91–99.

Maerz, N.H. & Zhou, W. 1998. Optical digital fragmentation measuring systems – inherent sources of error. *FRAGBLAST, The International Journal for Blasting and Fragmentation,* 2 (4): 415–431.

Maerz, N.H. & Zhou, W. 2000. Calibration of optical digital fragmentation measuring systems. *FRAGBLAST, The International Journal for Blasting and Fragmentation*, 4 (20): 126–138.

Palangio, T.C. & Maerz, N.H., 1999. Case studies using the WipFrag image analysis system. *FRAGBLAST 6, Sixth International Symposium For Rock Fragmentation By Blasting*, Johannesburg, South Africa, 8–12 August 1999, pp. 117–120.